

Geological carbon sequestration in the context of two-phase flow in porous media: A review

Luqman K. Abidoeye, Diganta B. Das[#], Kamal Khudaida

Department of Chemical Engineering, Loughborough University, Leicestershire,
LE11 3TU

Revised version submitted for review and publication in:

Critical Reviews in Environmental Science and Technology

Running paper title:

Geological carbon sequestration in the context of two-phase flow

5th May 2014

[#]Corresponding Author (Email: d.b.das@lboro.ac.uk; Tel: +44 (0)1509 222509)

1 **Geological carbon sequestration in the context of two-phase flow in porous**
2 **media: A review**

3
4 **Luqman K. Abidoeye, Diganta B. Das #, Kamal Khudaida**

5 Department of Chemical Engineering, Loughborough University, Leicestershire, LE11
6 3TU

7
8 #Corresponding Author (Email: d.b.das@lboro.ac.uk; Tel: +44 (0)1509 222509

9
10 **Abstract**

11 In this review, various aspects of geological carbon sequestration are discussed in
12 relation to the principles of two-phase flow in porous media. Literature reports on
13 geological sequestration of CO₂ show that the aquifer storage capacity, sealing integrity
14 of the caprock and the *in situ* processes, e.g., the displacement of brine by supercritical
15 CO₂ (scCO₂), convection-diffusion-dissolution processes involving scCO₂ and brine,
16 geochemical reactions, and mineral precipitation depend on the fluid-fluid-rock
17 characteristics as well as the prevailing subsurface conditions. Considering the
18 complexity of the interrelationships among various processes, experimental
19 investigations and network of mathematical functions are required for the ideal choice
20 of geological site with predictable fluid-fluid-rock behaviours that enhance effective
21 monitoring. From a thorough appraisal of the existing publications, recommendations
22 are made for improvement in the existing simulators to fully couple the entire processes
23 involved in the sequestration operations and *in situ* mechanisms which include injection
24 rate and pressure, brine displacement, simultaneous flow of free and buoyant phases of
25 CO₂, various trapping mechanisms, convection-diffusion-dissolution processes, scCO₂-
26 brine-rock reactions, precipitation of the rock minerals and the consequences on the
27 hydraulic and hydrogeological properties in the course of time as well as the quantity of
28 injected CO₂. Suggestion is made for the inclusion of leakage parameters on site-
29 specific basis to quantify the risks posed by the prevailing fluid-fluid-rock characteristics
30 as well as their immediate and future tendencies. Calls are also made for thorough
31 investigations of factors that cause non-uniqueness of the two-phase flow behaviour
32 with suggestions for the use of appropriate experimental techniques. The review
33 comprehensively synthesizes the available knowledge in the geological carbon
34 sequestration in a logical sequence.

36 **Keywords:** Carbon sequestration, global warming, capillary pressure, saturation,
37 relative permeability, dynamic effects, modelling and simulation.

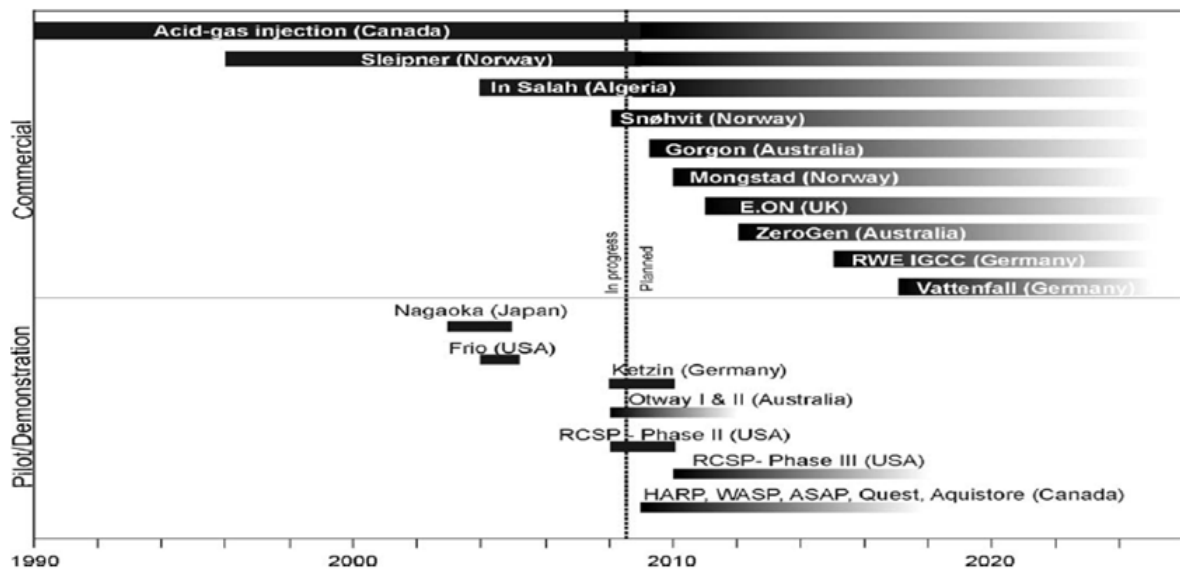
38

39 **1. Introduction**

40 The world is currently confronted with the issue of global warming arising mainly from
41 the anthropogenic activities, especially man's excessive use of fossil fuels for energy.
42 This has resulted in the unhindered emissions of several climate-unfriendly gases into
43 the atmosphere. There are significant evidence which has shown that these emissions
44 exacerbate the change in the climate by forming a blanket of gases which accumulate
45 at the lower part of the atmosphere, trapping the reflected radiation from the earth
46 thereby raising the surface temperature (Karl et al. 2009; Solomon et al. 2007). Owing
47 to the increasing amount of global emission, carbon dioxide is of serious concern as it
48 is considered to be the greatest culprit in the greenhouse effect (Metz et al. 2005;
49 Marland and Rotty 1984). Sources of these pollutants include, e.g., fossil fuels and
50 deforestation practises (Karl et al. 2009).

51

52 In the face of increasing global energy demands, the desire to mitigate the change in
53 climate presents a daunting and interesting challenge as ninety per cent of world's
54 primary sources of energy still comes from fossil fuels (DOE 2010). The world
55 population still hopes for an improvement in the standard of living, education and health
56 care. These aspirations are directly related to energy consumption. To check the steep
57 rise in carbon emission since the industrial revolution (200 to ~385 ppm) and preserve
58 the planet, CO₂ will need to be reduced to, at most, 350 ppm (Houghton et al. 2001;
59 Hansen et al. 2008). In tackling the challenges, various technologies have emerged
60 while many others are under investigations and implementations to reduce the
61 emissions of these gases into the atmosphere, utilise alternative energies, improve
62 carbon capture, or promote storage efficiencies and so on. Figure 1 shows the pilot and
63 commercial scale carbon sequestration projects being executed worldwide.



64
65 Figure 1: Carbon dioxide sequestration operations at pilot and commercial scales
66 worldwide (Michael et al. 2010).

67
68 Popular sites identified as suitable for carbon storage include ocean, brine or saline
69 aquifer, coal bed and depleted oil reservoir. However, the geological sequestration in
70 saline aquifers is considered as the most viable option as it seems to have the largest
71 carbon storage potential (Fujii et al. 2010; Zahid et al. 2011). Parts of the reasons for
72 this choice include the stability, capacity and ubiquity of these aquifers. Stable
73 sedimentary basins are necessary for dependable sequestration activities and such
74 basins are found in most continents (Metz et al. 2005) with estimated capacities of
75 around 1000 to 100,000 gigatonnes of carbon dioxide (Zahid et al. 2011). Researchers
76 have thus dedicated many studies to determine storage capacities and fluid flow
77 mechanisms at prospective sites. The ultimate choice of a particular geological site will
78 depend on a combination of several characteristics which include aquifer size, porosity,
79 permeability, depth, geology, hydrogeology, caprock integrity, petrophysical
80 characteristics, geothermal gradient, proximity to emission sources and existing
81 infrastructures, tectonic stability and faulting intensity (Espinoza et al. 2011).

82
83 Scenarios of the injected CO₂ in the brine aquifer for sequestration purposes involve
84 several in situ mechanisms, one of which is the displacement of the resident brine by
85 the invading CO₂ plume (Zhang et al. 2011; Juanes et al. 2006). Considering this as a
86 kind of two-phase system, multiphase flow researchers have delved into supercritical
87 CO₂-brine (scCO₂-brine) system with emphasis on capillary pressure-saturation-relative
88 permeability relationships ($P^c - S - K_r$) (Plug and Bruining 2007; Plug et al. 2006;

89 Pentland et al. 2011; Pini et al. 2012; Tokunaga et al. 2013). Capillary pressure and
90 relative permeability for wetting and non-wetting phases are parameters of key
91 importance in modelling the two-phase flow processes encountered during transport of
92 immiscible phases in the underground (Aggelopoulos and Tsakiroglou 2008) and they
93 constitute critical parameters used to history match and design field-scale injection
94 projects using reservoir simulators (Doughty 2007). Many publications are available on
95 the behaviour of P^c -S relationships (Hassanizadeh and Gray 1993; Mirzaei and Das
96 2007; Nordbotten et al. 2008; Bottero et al. 2011; Goel and O'Carroll 2011; Das et al.
97 2007) while several others are based on the K_r -S relationship (Bennion and Bachu
98 2008; Water et al. 2006; Lenormand et al. 1998; Anderson 1987). Most of these
99 publications consider the cases of oil-water and gas-water systems. So, it will be of
100 specific importance to thoroughly understand how the $P^c - S - K_r$ relationships behave
101 in $scCO_2$ -brine system.

102
103 For characterising $scCO_2$ -brine system in geological sequestration, two approaches are
104 most commonly considered. Firstly, it involves the use of the theories concerning
105 convection-diffusion-dissolution processes and secondly, it relates to the use of the
106 principles of two-phase flow in porous media. In the first case, the dissolution of the
107 $scCO_2$ in the aquifer brine is considered and it eliminates the need for determination of
108 capillary pressure. In this process, the carbon dioxide-brine solution is defined to be
109 slightly denser than the unsaturated brine causing negative buoyancy by moving to the
110 bottom of the aquifer, enhancing safe and permanent storage, which reduces chances
111 of leakage. The convective process promotes mixing of the brine and $scCO_2$ while
112 enhancing further dissolution of carbon dioxide into the brine (Ozgun and Gumrah 2009).
113 The second approach regards the supercritical carbon dioxide and brine as two
114 immiscible fluid phases, which can be described by $P^c - S - K_r$ relationships. This
115 assumes that there is a limited dissolution of CO_2 in the brine and that displacement
116 process dominates at least for some period after CO_2 injection.

117
118 To consider the $scCO_2$ -brine system as a two-phase flow system one requires the
119 understanding of the interactions of the fluid-fluid-porous media (i.e., gas-liquid-solid or
120 $scCO_2$ -brine-rock) in the system. Analogous to an oil-water system, the immiscible
121 displacement of $scCO_2$ -brine/water system may be affected by the presence of
122 heterogeneity in the media, viscosity and density ratios of the two fluids and the

123 geophysical as well as the geochemical conditions of the domain. For example, media
124 heterogeneities affect the $P^c - S$ and $K_r - S$ profiles (Das et al., 2004; Aggelopoulos and
125 Tsakiroglou 2008; Mirzaei and Das, 2013; Khudaida and Das, 2014) while they also
126 raise the value of the irreducible wetting phase saturation (Das et al. 2006). In addition,
127 the heterogeneity (e.g., fractures) may create preferential flow path which increases the
128 effective permeability of the fluid (Aggelopoulos and Tsakiroglou 2008). The
129 permeability to fluid is also affected by the presence of micron-scale heterogeneity (e.g.,
130 lamina) where varying intrinsic permeability value the degree of heterogeneity affect the
131 average permeability of the domain (Alabi 2011). These scenarios are important in the
132 choice of geo-sequestration sites as they affect storage capacity of the aquifer and can
133 influence the risks of leakage.

134
135 Recent review papers on CO₂ sequestration consider the alternative sequestration in
136 limestone (Stanmore and Gilot 2005), technologies and costs (Abu-Khader 2006),
137 health and safety issues (Zakkour and Haines 2007), analogy between traditional liquid
138 waste disposal and carbon storage (Tsang et al. 2007), storage in marine environment
139 (Huh et al. 2009), pilot projects (Michael et al. 2010), scCO₂-brine relative permeability
140 experiments (Müller 2011), caprock integrity (Shukla et al. 2010) and present and future
141 challenges (Zahid et al. 2011). Shukla et al. (2010) acknowledge the influences of the
142 fluid-fluid-media characteristics of the scCO₂-brine system on trapping mechanisms,
143 breakthrough of the injected fluid and capillary sealing of the caprock. Also, Müller
144 (2011) notes that while there are similarities in the measurement of relative permeability
145 for oil-water and CO₂-water systems, exception exists in the reactivity of core materials
146 with CO₂, resulting in permeability, porosity and wettability alteration. These pointed to
147 the unique characteristics of the two-phase flow parameters in the geological
148 sequestration processes. However, Shukla et al. (2010) are primarily concerned about
149 caprock integrity while Müller (2011) investigates the relative permeability experimental
150 methods.

151
152 To reliably predict CO₂ storage phenomena, understanding the capillary behaviour of
153 supercritical CO₂ and its dependence on water saturation are essential (Tokunaga et al.
154 2013). Characterising a system for geological storage of CO₂ also comes with the
155 challenges of dealing with high gas pressure and temperature above ambient
156 conditions as CO₂ is stored at a depth of around 1 km or more from earth's surface
157 (Rutqvist 2011). In addition to changing property of CO₂ at slight variation of conditions

158 in the subsurface, these scenarios might cause non-uniqueness in the functional
159 representation of the system such as those discussed by Das et al. (2006).

160
161 The above discussions introduce the practices of geological sequestration and the
162 relevance of two-phase flow (scCO₂-brine) parameters. It is however equally important
163 to illustrate the challenges and trends found in the literature concerning the
164 determination, application and interpretation of relevant two-phase flow parameters in
165 relation to the carbon sequestration processes. In addressing these issues, this review
166 intends to examine the research activities relating to geological sequestration of CO₂
167 together with the issues involved in the determination of two-phase relationships for
168 scCO₂-brine system from experiments, modelling and simulations. How scCO₂-brine-
169 rock characteristics affect stability/instability of the system will be extensively discussed
170 and suggestions as well as recommendations will be made in view of the identified
171 gaps in knowledge. This work is based on the up-to-date reliable information available
172 in the open literature

173

174 **2. Characteristics of the geological sites**

175 Geological sites hold the important properties that determine a successful geological
176 CO₂ sequestration projects. In this regards, the geological media should meet some
177 fundamental conditions to ensure successful storage of carbon dioxide. Three of these
178 are capacity, injectivity and confinement (Gunter et al. 2009). Studying and modelling
179 CO₂ sequestration in geological formation need a clear understanding of multi-phase
180 flow characteristics and their behaviour in porous media. The above-mentioned
181 parameters (i.e., aquifer capacity, injectivity and confinement) bear relation to media
182 properties i.e., porosity, tortuosity, permeability, relative permeability, dispersion
183 coefficient, capillarity, connectivity, adsorption and wettability as well as to two-phase
184 flow characteristics in the medium. Some of these media properties in the context of the
185 studies on CO₂ sequestration are discussed below.

186

187 **2.1 Porosity and pore size distribution**

188 In their review of characteristics of potential geological formations for CO₂ sequestration,
189 Kopp et al. (2009) explain that geological formations are suitable for carbon dioxide
190 storage if they demonstrate high values of porosity and permeability. These are crucial
191 for storage of high amounts of carbon dioxide and allow its injection to be done
192 economically.

193
 194 Porosity is the fraction of the aquifer that is composed of voids (Bear 2013). The
 195 interconnected voids in the aquifer forms what is referred to as the effective porosity
 196 and it determines the effective storage capacity of the aquifer. Chadwick et al. (2008)
 197 suggest that the amount of CO₂ that can be stored in a given saline aquifer in terms of
 198 a capacity factor C is:

$$200 \quad C = C^{\text{gas}} + C^{\text{liquid}} \quad (1)$$

201
 202 Where $C^{\text{gas}} = \langle \phi \cdot S_g \rangle$, $C^{\text{liquid}} = \langle \phi \cdot S_l \cdot X_1^{\text{CO}_2} \cdot \rho_l / \rho_g \rangle$ and C is the volume fraction of the
 203 reservoir available for storage. C is taken as the sum of the free supercritical CO₂ (C^{gas})
 204 and CO₂ dissolved in the brine (C^{liquid}). ϕ is the effective domain porosity and, S_l and S_g
 205 are the fractional volumes of the pore space containing liquid and scCO₂ phases,
 206 respectively. $X_1^{\text{CO}_2}$ refers to the mass fraction of dissolved CO₂ in the brine, ρ_g and ρ_l
 207 are the densities of the scCO₂ and liquid phases, respectively. The angle brackets
 208 imply averaging over the spatial domain of storage. Equation 1 shows that the porosity,
 209 ϕ , plays a very important role in determining the capacity factor of an aquifer and it can
 210 serve as a factor to check suitability of an aquifer for storage. According to Espinoza et
 211 al. (2011), the volume of CO₂ injected, V_{CO_2} , in an aquifer is a function of average
 212 aquifer porosity as follows:

$$214 \quad V_{\text{bulk}} = \frac{V_{\text{CO}_2}}{\phi} \frac{1}{\Psi} \quad (2)$$

215
 216 Where Ψ is a water or brine displacement efficiency coefficient and it is a function of
 217 the media and process characteristics. In essence, the effective porosity of an aquifer
 218 is a key factor in its capacity to store CO₂. According to Chadwick et al. (2008) a
 219 porosity greater than 20% is a positive indicator in a site selection while a value lesser
 220 than 10% porosity calls for caution. The porosity of sediment tends to decrease with
 221 depth as the effective stress on the sediment increases. The pore size and structure
 222 of an aquifer tend to change under the same influence as the pore size is a function of
 223 porosity and specific surface. Also, due to enormous complexity of the pore structure
 224 of any porous media in terms of the number of pores, their size, shape, orientation,
 225 and manner of interconnection of the pores, it often becomes important to consider

226 the pore size distributions of an aquifer. The pore size distribution is defined as a
227 fraction, f , of total pore spaces within a range of pore diameter δ and $\delta+d\delta$ as
228 expressed in the following distribution function:

$$229 \int_0^{\infty} f(\delta) d\delta = 1$$

230 (3)

231
232 Information concerning the pore size distribution of a particular aquifer can be
233 obtained from analysis of core measurements and even geophysical logs of adjacent
234 wells. In such sample, the P^c required to force a liquid (e.g., mercury) into the pores
235 can be used to approximate δ , with the following equation (Bear 2013):

236

$$237 \delta = 4\gamma \cos\theta / P^c$$

238 (4)

239

240 where, γ is the interfacial tension between the two fluids and θ is the contact angle.
241 Pore size distributions are useful in the analysis of permeability reduction, e.g., as a
242 result of clay swelling, microbial growth in pores, mineral precipitation, etc., (Tiab and
243 Donaldson 2004). Theory for the penetration of non-wetting fluid into the pore was
244 developed by Ritter and Drake (1945) while Burdine et al. (1950) applied it to study
245 two-phase flow in reservoir rocks. In the absence of typical mercury injection
246 information, pore size distribution information can be obtained from measurements
247 made by porous semi-permeable diaphragm method (Burdine 1953). Other methods
248 for determining pore size distribution, e.g., adsorption isotherm (Dollimore and Heal
249 1964; Seaton and Walton 1989) and induced polarization logging measurements
250 (Vinegar and Waxman 1987) have been reported as well. Information on pore size
251 distribution is important in the characterization of the displacement of brine by $scCO_2$
252 in the saline aquifer as it can be used to calculate the relative permeability of the
253 phases (Burdine 1953).

254

255 Changing porosity, mineral precipitation, dissolution and change in effective stress are
256 some of the factors that result in the evolution of pore size distributions of a reservoir.
257 Mineral precipitation in the porous media is often affected by pore size (Emmanuel et
258 al. 2010) and vice versa. While the large pores permit ready precipitation of minerals,
259 the smaller pores might inhibit the process leading to reduced bulk reaction rate,

260 which in effect stabilises the porosity. Also, geochemical reaction with rock minerals is
261 considered to be one of the trapping mechanisms for long term sequestration. The
262 pore lengths and their distribution might affect how readily the reactions occur at
263 different parts of the sediment. Precipitation of quartz was found to be inhibited in
264 pores smaller than 10 μm in diameter. Also, the pore size distribution will also affect
265 the dissolution rate which is another mechanism identified for trapping as varying
266 solubility is applicable (Emmanuel et al. 2010). In addition, the standard deviation of
267 pore size distribution affects CO_2 breakthrough into a medium (Espinoza et al. 2011).

268

269 **2.2. Intrinsic, Relative and Effective Permeability**

270 Permeability, as the name suggests, is an indication of how easily a fluid will pass
271 through a porous medium. It can be defined by Darcy's law (Bear 2013; Virnovsky et al.
272 1995) for an incompressible fluid having viscosity, μ , which flows through a porous
273 medium with length, L , and cross sectional area, A , at flow rate, q , and pressure
274 difference of ΔP across the domain. The isotropic permeability, K , of the porous
275 medium is defined as:

276

$$277 \quad K = \frac{q\mu L}{A\Delta P}$$

278 (5)

279

280 Its value is dependent on the porous structure of the medium. Appropriate permeability
281 needs to be maintained in the medium to ensure effective storage of CO_2 (Rutqvist
282 2012). However, the permeability of a medium is affected by the reactions, dissolution
283 and precipitations of the rock minerals. Simulations have shown that following CO_2
284 injection, dissolution of carbonate cement initially increases the sediment porosity but
285 subsequent reactions result in dissolution of feldspar and precipitation of carbonate
286 minerals and clay leading to reduction in permeability and porosity (Gaus et al. 2005).
287 This implies that the original permeability of the sediment may alter in the course of
288 injection and will affect the prediction of the process behaviour.

289

290 Meanwhile, the flow processes (like that in geological sequestration system) can hardly
291 occur with a single fluid. This reality leads to the concept of relative permeability that
292 represents the two-phase relationships of scCO_2 -brine system in a geological media.
293 While the permeability is the intrinsic property of the medium, relative permeability is

294 the characteristic of the fluid-fluid-solid system and it comes to play when two or more
295 fluids are present in the porous medium. The term describes the extent to which one
296 fluid is hindered by the other. Though relative permeability is dependent on a number of
297 factors, available experimental evidence indicates the concept of relative permeability
298 that depends on only saturation is a good approximation for all practical purposes (Bear
299 2013). It is expressed through Darcy's law set up for individual phase i that flows in the
300 pore space:

301

$$302 \quad q_i = \left(\frac{KK_{ri}}{\mu_i} \right) A \frac{\Delta P_i}{\Delta x}$$

303 (6)

304

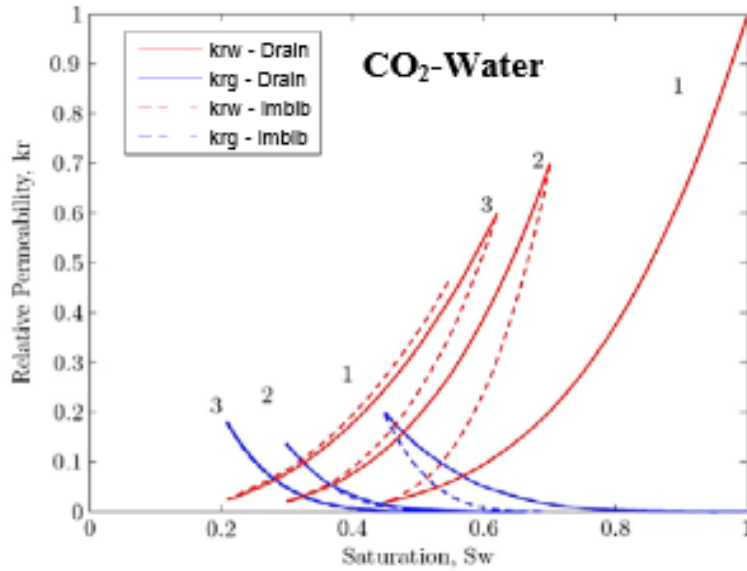
305 q_i , K_{ri} , μ_i , and ΔP_i refer to the flow rate, relative permeability, viscosity and the pressure
306 drop, respectively for phase i . The ratio $\left(\frac{KK_{ri}}{\mu_i} \right)$ denotes the "mobility" of phase i .

307 Figure 2 shows the relative permeability plots of CO₂-water system. It consists of
308 primary, secondary and tertiary drainage of the system (see, Bear (2013) for definitions
309 of these processes). It can be seen that following primary drainage, the residual water
310 saturation continues to decrease in subsequent drainages. This is attributed to
311 dissolution property of CO₂ in water and a contrast was shown in N₂-water system
312 which shows a fairly similar residual saturation for the subsequent drainages owing to
313 lesser solubility of N₂ (Pistone et al. 2011). Water relative permeability, K_{rw} is higher for
314 larger portion of the water saturation though the value reduces with subsequent
315 drainages while that of CO₂ remains low. Relative permeability of CO₂, K_{rg} , remains low
316 owing to dissolution and diffusion into smallest pore spaces with no need to overcome
317 the entry pressure. Evolution of CO₂ from this dissolution state displaces previously
318 immobile water which further impedes CO₂ mobility (Pistone et al. 2011). Thus, the
319 residual saturation of water continues to reduce following subsequent drainage.

320

321 Bickle et al. (2007) concluded that the relative permeability-residual saturation relations
322 have a great influence on average carbon dioxide saturation as well as plume evolution
323 velocity and as such, have a great effect on storage capacity. Hysteresis in relative
324 permeability has the tendency to enhance residual trapping. This is defined, for a
325 particular CO₂ saturation, as a reduction in relative permeability during imbibition

326 compared to drainage (Chadwick et al. 2008). Strong hysteresis in relative permeability
 327 results in 'sticky' plumes that leave behind relatively higher amounts of CO₂ trapped
 328 compared to weak hysteresis leaving behind small amount. This scenario was
 329 observed in the simulation of sequestration project at Sleipner (Norway) (Chadwick et al.
 330 2008).



331
 332 Figure 2: Relative permeability curves for CO₂ (blue) and water (red) (Pistone et al.
 333 2011).

334
 335 On the basis of a large number of drainage experiments with various types of media,
 336 Brooks and Corey (1964) suggest the following relative permeability function:

$$337 \quad k_{rw} = (S_e)^{(2+3\lambda)/\lambda} = \left(\frac{P_b}{P^c}\right)^{(2+3\lambda)} \quad P^c \geq P_b$$

338 (7)

$$339 \quad k_{mww} = (1 - S_e)^2 (1 - S_e^{(2+\lambda)/\lambda}) = [1 - (P_b/P^c)^\lambda]^2 [1 - (P_b/P^c)^{2+\lambda}]$$

340 (8)

341
 342 where λ is the pore-size distribution index, P_b is referred to as the bubbling or threshold
 343 pressure or entry pressure. S_e is the effective saturation and can be expressed as
 344 $S_e = (P_b/P^c)^\lambda$ for $P^c \geq P_b$. Even though the above results are deduced for isotropic
 345 media, their validity makes them applicable to a wide range of pore-size distributions
 346 (Bear 2013). Several factors can affect the effective permeability of an aquifer. Pore
 347 size distributions, media heterogeneities and scale can be of considerable impact. This

348 was corroborated by Alabi (2011) investigating the difference in the flow rate of fluid in
349 homogeneous media and different types of heterogeneous media. The author found out
350 that the permeabilities of heterogeneous media are lower than the permeabilities of
351 homogeneous media and that mixed heterogeneity has higher permeability than
352 layered type. This implies that fluid flows faster in mixed heterogeneous sample than
353 the layered type.

354

355 **2.3 Threshold pressure (bubbling pressure)**

356 In scCO₂-brine system, the pressure in the invading fluid (i.e., scCO₂) at the interface
357 between fluid-fluid and rock system is required to exceed the minimum entry pressure
358 of the sediment. This implies a certain pressure must be reached in the non-wetting
359 fluid before it begins to penetrate the sample, displacing the wetting fluid contained in it
360 (Bear 2013). The minimum pressure needed to initiate this displacement is called the
361 threshold pressure (or bubbling pressure) or non-wetting fluid entry value or
362 breakthrough pressure. This parameter is also a pointer to injectivity of a medium and
363 its excessive magnitude can pose serious risk to the caprock.

364

365 Understanding of the threshold pressure of a caprock saturated with water is important
366 when a gas is to be stored in the reservoir underneath the caprock. This is also the
367 breakthrough pressure when CO₂ can enter through the caprock. Its value depends on
368 the mean pore size related to specific surface S_s, standard deviation in pore size
369 distribution and void ratio e as well as the wettability of the minerals in the presence of
370 water and CO₂ (Espinoza et al. 2011); $e = e_{1kPa} - C_c \log(p'/1kPa)$ where p' is the *in situ*
371 effective stress and e_{1kPa} is the critical state void ratio when the mean confining stress
372 is 1kPa. Espinoza and Santamarina (2010) gave expression for breakthrough pressure,
373 P_{thru}^{*}, by extension of Laplace's capillary pressure equation:

374

$$375 \quad P_{thru}^* = \Psi \frac{S_s \rho \gamma \cos \theta}{e}$$

376 (9)

377

378 Ψ is a factor that depends on the clay fabric and grain size distribution and a value of
379 0.04<Ψ<0.08 applies to smectite clay barriers and, γ is the interfacial tension. This
380 interfacial tension is an important property of the two-phase system. Its influence

381 depends on the prevailing conditions, e.g., temperature, pressure, salinity and cation
382 valence. Detail discussions and the implication of these factors on γ will be found
383 under subsection 5.2 in this work.

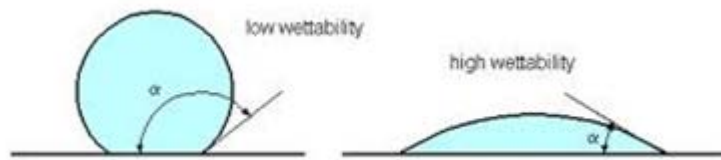
384

385 Aside the sediment where actual injection and storage occur, threshold capillary
386 pressure is an important parameter of the caprock that gives indication about its sealing
387 capacity or integrity of caprock. It combines with caprock permeability to determine
388 possibility of leakage and its rate of occurrence (Fleury et al. 2010; Pusch et al. 2010).
389 Thus, the threshold pressure for the sediment must be well below that of the caprock to
390 avoid undue development. Also, since the injection and the *in situ* displacement
391 processes result in pressure fluctuations within the system, the caprock entry pressure
392 should be well in excess of any possible pressure increase for long-term safety.
393 Practical caprock core from Sleipner (Norway) was reported to possess greater than
394 3.3 MPa capillary entry pressure to scCO₂ while that of another project from Schwarze
395 Pumpe (Schweinrich) is predicted to be in the range 4 to 40 MPa (Chadwick et al.
396 2008).

397

398 **2.4 Wettability**

399 Wettability is the ability of a liquid to adhere to a solid surface due to their
400 intermolecular interactions. It has a significant impact on the relative permeability-
401 saturation relationships and can be determined from the combination of cohesion forces,
402 which cause the drop to prevent contact with the solid surface, and adhesion forces that
403 try to spread the liquid across the solid surface in a flow system. It is among the factors
404 that determine the entry pressure of the geological media (Espinoza et al. 2011). If the
405 medium is CO₂-wet, it becomes easier for the invading CO₂ to displace the resident
406 brine. However, if the medium is water-wet, then higher entry pressure is required for
407 the invading CO₂ to penetrate the medium. Publications on water-wet, CO₂-wet and
408 mixed-wet media have been reported. In relation to carbon geological sequestration,
409 many of the representative media samples, quartz, calcite, kaolinite, microcline and illite
410 were reported to be water-wetting (Wang et al. 2012). The possibility of the alteration in
411 wettability based on saturation history of the medium was also reported (Plug et al.
412 2006).



413
 414 Figure 3: Wettability index of liquid as a function of contact angle (α): $\alpha > 90^\circ$ (non-
 415 wetting liquid), $\alpha < 90^\circ$ (wetting liquid). The possibility of $\alpha=0^\circ$ (perfectly wetting) is not
 416 shown.

417
 418 Wettability is related to capillary effects and occurs at different degrees according to the
 419 angle at which fluid1-fluid2 interface meets with the fluid1-solid interface. This contact
 420 angle provides an inverse measure of wettability (Shafrin and Zisman 1960).
 421 Importance of wettability in the determination of $P^c - S - K_r$ relationships is great and
 422 the *in situ* alteration in wettability can lead to error in calculation and predictions if not
 423 considered. Wettability indices (e.g., USBM index, Ammott index and Hammervold-
 424 Longeron (HL) index) are employed in quantifying wettability and its changes for the
 425 drainage and waterflooding processes in the porous media using the P^c -S curves
 426 (Pentland 2011). Table 1 shows the wettability indices for oil–water system.

427
 428 Table 1: Wettability indices for oil-water indices (Pentland 2011)

Index	Water-wet	Neutrally-wet
Oil-wet		
Ammot	Positive	0
(displacement by water ratio)		0
Hammervold-Longeron	1	-1
USBM	near 1	near 0
near -1		

429
 430 By implication, partial-wetting behaviour of CO_2 (e.g., limestone rock under reservoir
 431 condition) results in lower capillary pressure and higher mobility for brine and can lead
 432 into lower capillary breakthrough pressure of the caprock (Chalbaud et al. 2010).

433
 434 **3. *In situ* Trapping Mechanisms of Injected CO_2**

435 Trapping mechanisms come under two major categories: physical and chemical
 436 trapping mechanisms. Physical mechanism involves the trapping by structural and

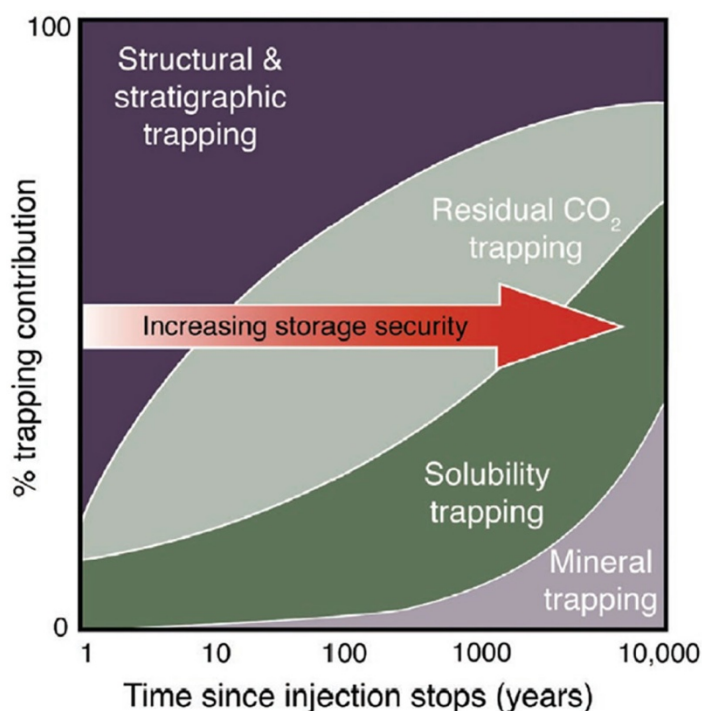
437 stratigraphic patterns of the aquifer sediment and caprock while chemical mechanisms
438 include dissolution in the brine, complex mineralisation with host rock, adsorption on
439 coal and CO₂ hydrate formation (Espinoza et al. 2011). Some of these trapping
440 mechanisms are discussed below under the broad headings of structural, dissolution,
441 capillary and mineral trapping.

442

443 3.1 Structural trapping

444 Structural trapping arises from physical nature of the aquifer, e.g., anticlines or faults
445 intercepting the upward mobile plume of CO₂. Together with stratigraphic as well as
446 hydrodynamic trappings, they constitute physical trapping mechanisms that control the
447 initial period of CO₂ storage (White et al. 2001). Structural trapping occurs in the
448 presence of a structural enclosure together with a seal forming low permeability cap-
449 rock (Omambia and Y. Li 2010). The injected carbon dioxide rises to the upper layer of
450 the aquifer above the resident brine by the power of buoyancy and is immobilised under
451 the impermeable anticline structure. In a sequestration project at Sleipner (Norway)
452 structural traps are the key features focused upon prior to CO₂ injection as they are key
453 to favourable geological site characterisation (Chadwick et al. 2008). From 1996, the
454 CO₂ plume had reached the top of the reservoir by 1999 at Sleipner (Shukla et al.
455 2010). Figure 5 depicts this mechanism in a reservoir as CO₂ trapped under caprock.

456



457

458 Figure 4: Mechanisms of CO₂ Trapping with time (Benson and Cole 2008).

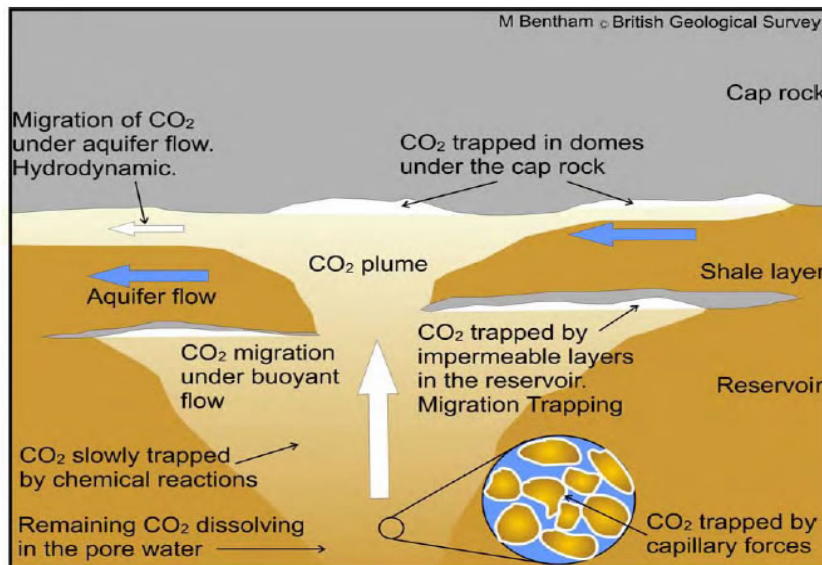
459

460 3.2 Residual trapping

461 Residual trapping occurs as a result of a hysteresis effect in the permeability of the
462 scCO₂ phase especially when the saturation direction is reversed. It is a quick process
463 because of the tight and rigid sponge nature of the porous rock (Omambia and Li 2010).
464 As the scCO₂ is injected into the deep aquifer formation, it displaces the resident fluid.
465 When the scCO₂ continues to move, the previous brine takes its place trapping some of
466 the scCO₂ adhered to the pore surface and stay behind trapped in the pore spaces as
467 residual droplets rendered immobile like water in a sponge (Ide et al. 2007). It is
468 depicted in Figure 5.

469

470 The trapping of a phase in this manner can be characterised by the relationship
471 between initial and residual saturation, known as the capillary trapping curve. This
472 phenomenon can be characterised by maximum trapped saturation and the form of the
473 capillary trapping curve as these depict the physics of this phenomenon and also give
474 an important indication of system wettability.



475

476 Figure 5: Various mechanisms of CO₂ trapping in the reservoir (Bentham 2006)

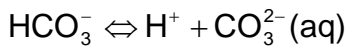
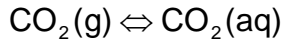
477

478 3.3 Solubility trapping

479 It is envisaged that the long-term sequestration of CO₂ in deep saline aquifers will occur
480 via dissolution in the brine and/or chemical complexation with the formation (White et al.
481 2003). Solubility trapping occurs when CO₂ in gaseous or supercritical state dissolves in
482 the aquifer brine at the prevalent conditions of temperature, salinity and pressure
483 (Omambia and Y. Li 2010). This results in the increase of the solution density and

484 lowered pH as shown in Figure 6. As the CO₂ dissolves in water, part of this mixes with
 485 the water and form the carbonic acid which goes on to produce bicarbonate with
 486 hydrogen ions. This reduces the pH of the system at reservoir conditions to
 487 approximately 3. The following steps represent the ionization process:

488



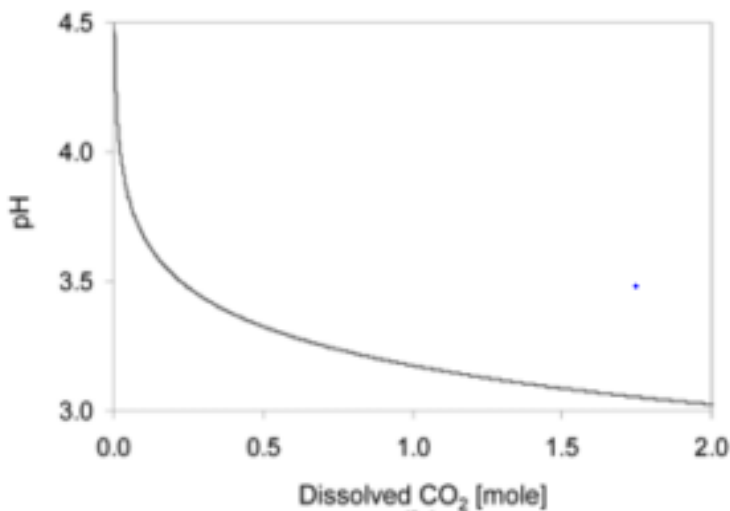
490

491 Being heavier than other surrounding fluids as a result of the dissolved CO₂, convective
 492 currents are created causing the denser solution to settle at the bottom of the aquifer
 493 trapping the CO₂ more securely. The lighter brine with less dissolved CO₂ then rises to
 494 the top of the rock formation (Silin et al. 2008). The mass density of brine-CO₂ solution,
 495 ρ_{sol} (kg/m³), can be estimated from equation (11) (Espinoza et al. 2011):

496

$$497 \quad \rho_{\text{sol}} = \rho_w + m_{\text{CO}_2} \chi_{\text{CO}_2} - \chi_{\text{CO}_2} \rho_w V_\phi$$

498 (11)



499

500 Figure 6: Solution pH as a function of solubility of CO₂ in brine (Duan and Sun 2003).

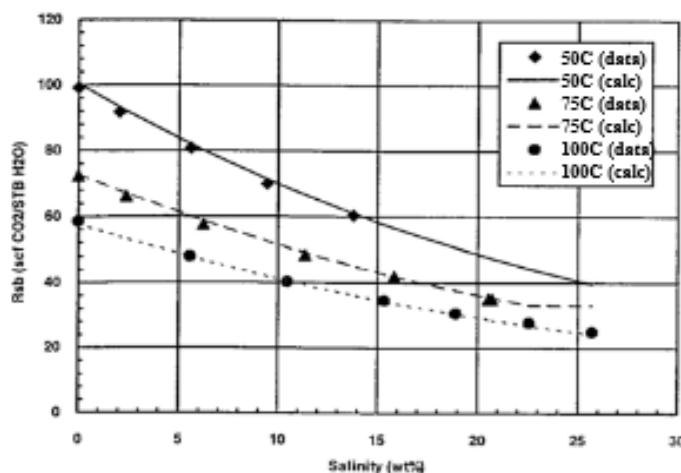
501

502 ρ_w (kg/m³) is the density of pure water, χ_{CO_2} (mol/m³) is the CO₂ concentration in water,
 503 m_{CO_2} (kg/mol) is the molecular weight of CO₂, V_ϕ (m³/mol) is the apparent molar volume
 504 of CO₂ as a function of temperature, T(C) expressed by Garcia (2001) as
 505 $V_\phi = 37.51 \cdot 10^{-6} - 9.585 \cdot 10^{-8} T + 8.740 \cdot 10^{-10} T^2 - 5.044 \cdot 10^{-13} T^3$. Densification of the

506 brine-CO₂ solution promotes the convective mixing in the aquifer, which improves the
 507 effectiveness of this trapping mechanism. This continues until the system reaches
 508 equilibrium condition.

509
 510 Solubility is affected by the temperature and pressure of the system, pore size
 511 distribution. So, the choice of basins with higher density of large pores will aid this
 512 mechanism (Emmanuel et al. 2010). The dissolution increases with pressure and
 513 decreases with temperature as shown in the chart presented by Dodds et al. (1956)
 514 with different patterns of dissolution below and above critical conditions. Also, salt
 515 concentration of the brine has been shown to affect the solubility of CO₂. There appear
 516 to be an indirect linear relationship between CO₂ solubility and salt concentration as
 517 shown in Figure 7. This implies that aquifer with lower brine concentration favor s this
 518 dissolution mechanism.

519
 520 A dimensionless number, namely, Rayleigh number (Ra) is important in the dissolution-
 521 convection processes involved in the solubility trapping. Ra is particularly associated
 522 with buoyancy-driven flow. It is dependent on the fluid property and the characteristic
 523 length of the system expressed as (Farajzadeh 2009): $Ra = \frac{\beta_c g \Delta c R^3}{\nu D}$. β_c is the
 524 volumetric expansion coefficient (m³/mol), g is the acceleration due to gravity (m/s²), c
 525 is the gas concentration (mol/m³), R is the characteristic length of the system (m), ν is
 526 the kinematic viscosity (m²/s) and D is the diffusion coefficient (m²/s). As Ra increases
 527 mass transfer of CO₂ into the brine-saturated porous medium increases and the
 528 concentration front moves faster (Farajzadeh 2009). Low Ra results into the steady-
 529 state concentration while its high value leads to the system instability (Ouakad 2013).



530

531 Figure 7: CO₂ solubility as a function of salinity (Chang et al. 1998)

532 .

533 **3.4 Mineral trapping**

534 When carbon dioxide is dissolved in brine, it decreases the pH of the solution leading to
535 acidification as expressed in equation (10). This acidified solution in contact with host
536 rock results in mineral dissolution, precipitation and reactions, which are the processes
537 that induce mineral trapping. With time, the reactions of the acid with dissolved ions and
538 rock minerals in the aquifer lead to chemical complexes such as magnesite, dolomite,
539 calcite, drawsonite and siderite. These occur as products of dissolution and complexing,
540 resulting in chemical precipitation of solid carbonate minerals (secondary carbonates).
541 It is regarded as a permanent sequestration process. However, it is a slow process with
542 significant contribution occurring only in the geological time scale.

543

544 Reaction between CO₂ and alkali aluminosilicate minerals will generate a soluble alkali
545 bicarbonates as well as carbonates promoting the mechanism of solubility trapping. In
546 this line of series, parallel and complex reactions and processes, pH of the system
547 changes dramatically as the dissolution of carbonates ions raises it up to 5 while
548 aluminosilicates can take the pH up to 8 (Espinoza et al. 2011).

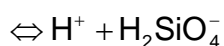
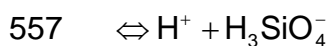
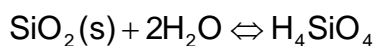
549

550 Beni et al. (2012) evaluated the potential of mineral trapping on CO₂ sequestration in
551 the sandstone formation near Minden in Germany. They found that after about 200
552 years, this mechanism contributes significantly in the storage and the prospect
553 increases even more with time.

554

555 Typical reaction with silicate mineral is represented below (Drever and Stillings 1997):

556



558 (12)

559 Equation (12) has a reaction rate of $1.26 \times 10^{-14} \text{ mol.m}^{-2}.\text{s}^{-1}$ (White et al. 2004) and the
560 reaction is not affected by dissolution of CO₂. But the reaction with aluminosilicates
561 (including feldspars, micas, clays) turns the system alkaline with pH up to 8 (Li et al.
562 2006) while faster carbonate reactions raise the pH up to 5 (Algive et al. 2009).

563

564 4 Modelling and simulations of scCO₂-brine-rock system

565 Modelling and simulations of geological sequestration processes are highly required to
566 assess the feasibility of CO₂ sequestration into particular aquifer or reservoir. Modelling
567 the sequestration entails considerations for the technicalities of the storage systems
568 and the economics. This ranges from capture, transport and storage together with the
569 associated costs brought together in a discounted cash flow calculations (Chadwick et
570 al. 2008). However, the interest of this section is to discuss the basics of modelling and
571 simulations involved in geological sequestration.

572 Generally, the geological sequestration systems can be described using multiphase
573 and multi-component processes with consideration for non-isothermal conditions
574 occurring near the injection region owing to CO₂ expansion with Joule-Thompson
575 effects (Class et al. 2009). Basic multiphase equations are built upon mass and
576 momentum conservations as well as various constitutive equations. For the
577 simultaneous flow of CO₂ and water, the governing equations can be expressed as:

578

$$579 \quad \phi \frac{\partial S_i}{\partial t} + \nabla \cdot q_i = 0$$

580 (13)

581

582 'i' stands for the phases; CO₂ (g) or brine/water (w). S is the phase saturation and q the
583 velocity and ϕ , the porosity. . The velocity q is given by the extended version of Darcy's

584 law; $q_i = -\frac{K_{ri}K}{\mu_i}[\nabla P_i + \rho_i g \nabla z]$. For radial injection in the aquifer (Saripalli et al. 2001);

585 $q_{r,i} = \frac{Q_i f_i(S_i)}{2\pi r h}$. $K_{r,i}$ represents the relative permeability for phase i and K is the medium

586 intrinsic permeability. P is the phase pressure, ρ the density and g is the acceleration
587 due to gravity, ∇z is the gradient of upward unit vector. Q is the injection rate and f is
588 the phase fractional flow. For the injected phase, substituting for radial velocity in
589 equation (13) results into two-phase displacement theory based on the Buckley-
590 Leverette theory (Saripalli et al. 2001):

591

$$592 \quad \frac{Q_g f_g}{2\pi r h \phi} \frac{\partial S_g}{\partial r} + \frac{\partial S_g}{\partial t} = 0$$

593 (14)

594

595 In addition to the above, a detailed description of the constitutive equations for the
596 sequestration system requires several mathematical expressions which include the CO₂
597 saturation in the expanding radial plume and its derivative, equation of state for the
598 phase partitioning behaviour of CO₂-H₂O mixture, models for dissolution of CO₂ in brine
599 and vice versa with their derivatives along the horizontal and vertical regions and
600 pressure distribution in the region of the plume. While the radial flow of the injected
601 phase is inserted as velocity in the equation (14) (Saripalli et al. 2001), the buoyant flow
602 of the process needs a separate velocity expression as a function of radius.
603 Furthermore, incorporating expressions for leaks is desired for robust modelling and
604 analysis of injection and sequestration processes.

605
606 For CO₂ leaks scenarios, two significant processes are of concern: vertical migration as
607 a free phase through fractures and buoyancy driven flow through permeable zones of a
608 water-saturated caprock were identified (Huo and Gong 2010; Saripalli et al. 2001).
609 Young-Laplace relation for capillary pressure provides a handy expression for
610 determining the entry capillary pressure from the values of two-phase interfacial tension
611 and pore size obtained for the caprock (Singh et al. 2010). Thickness of the CO₂ bubble
612 layer near the caprock will provide the needed parameter for the exerted pressure on
613 the confinement and expression for free phase flow of CO₂ through the aperture is
614 required for the complete description of the leak scenario. In very robust case,
615 incorporating chemical reactions from dissolution, mineral precipitations, various
616 trapping mechanisms are highly desired. The above scheme can be simplified for easy
617 solution depending on the level of analysis desired but the more processes that are
618 incorporated into the model the better the simulation and the more robust and better its
619 application. This calls for the assessment of the currently available simulators. Though,
620 it is recognised that the solution methods become complicated with complex multi-
621 process models.

622
623 Popular approaches to the solution of mathematical modelling are analytical, semi
624 analytical and numerical techniques. For example, Woods and Comer. (1962) obtained
625 analytical solution to equation (14) for radial injection of gases into initially water-
626 saturated reservoir. Similarly, Nordbotten et al. (2005) provide analytical solution to the
627 space-time evolution of CO₂ plume. However, for very complex problems, non-linearity
628 in constitutive relations often defies analytical solution. As such, numerical solution is
629 often applied. Numerical solution allows simulations that incorporate diverse injection

630 wells with varying injection rates, heterogeneous geologic formations, and simultaneous
631 chemical reactions as well as mass transfer processes. If sufficient data are available,
632 achievable CO₂ saturation, local or regional pressure constraints, dissolution as well as
633 residual saturation can be assessed with numerical simulation as they are dependent
634 mainly on the reservoir and fluid properties as well as injection strategies (Chadwick et
635 al. 2008).

636
637 Software designed for hydrocarbon systems in the oil industries are easily adaptable to
638 CO₂ storage as evident by code inter-comparison study (Pruess et al. 2003). However,
639 currently many numerical simulators have emerged in the field of sequestration
640 processes with function-specific as well as general applications. They include NUFT-
641 SYNEF (Morris et al. 2011a; Morris et al. 2011b), STOMP (White 2002), FEMH (Bower
642 and Zyvoloski 1997), ECLIPSE-VISAGE (Ouellet et al. 2011), OpenGeoSys (Wang and
643 Kolditz 2007), TOUGH2 (Pruess et al. 1999), TOUGHREACT (Xu et al. 2006), TOUGH-
644 FLAC (Rutqvist 2011; Rutqvist et al. 2002), CODE-BRIGHT (Olivella et al. 1994;
645 Vilarrasa et al. 2010), DYNFLOW (Preisig and Prévost 2011), STARS (Bissell et al.
646 2011). Also, COORES, DuMux, GPRS, MUFTE, MoReS, ROCKFLOW and ELSA are
647 some of the models with capability for simulating different carbon sequestration
648 scenarios and are involved in the benchmark study for the inter comparison of
649 mathematical and numerical models in the context of geological carbon sequestration
650 (Class et al. 2009). In some (e.g., TOUGHREACT) fluids and heat flows are coupled
651 with reactive geochemistry to enhance applications in geological carbon sequestration.

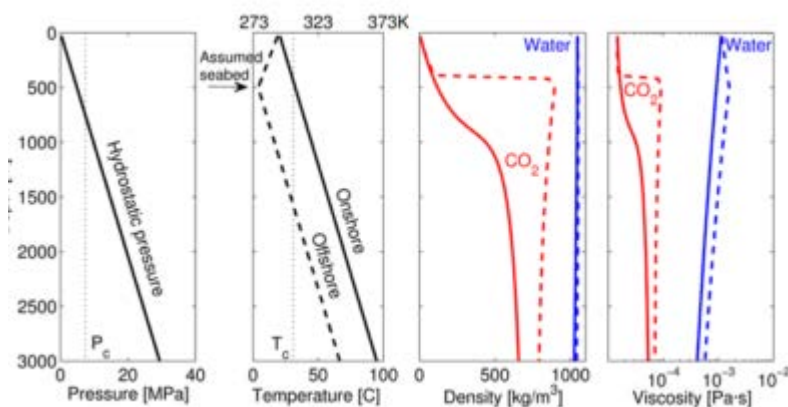
652
653 The simulation code, 'subsurface transport over multiple phases (STOMP)' developed
654 using advance computational tools by Pacific Northwest National Laboratory (PNNL,
655 Washington) has the ability for simulating fully coupled mass and heat transport with
656 kinetic and/or equilibrium controlled chemical reactions, temporal and spatial responses
657 to injection, injectivity, hydrogeological and fluid properties change (White and McGrail
658 2005). Class et al. (2009) emphasised the investigation of influence of gridding, model
659 concepts and mechanisms to ensure quality control and assessment of numerical
660 simulators. However, further developments are required in the ability of the simulators
661 to quantify and relate leak factors on a site-specific basis. This should establish the
662 threshold values that may compromise the reservoir integrity. For example, one needs
663 to determine what quantity of CO₂, in conjunction with gas-brine-rock interactions and
664 time will result in leakage. Ability to easily predict this scenario will afford the

665 researchers the opportunity to establish site-specific limit of injection. For example, the
 666 work of Schwartz (2014) using TOUGHREACT presented a leakage factor:
 667 transmissibility. This was established for a potential leak zone as a product of width and
 668 permeability with a threshold value of $1.7 \times 10^{-3} \text{ m}^3$. This is established based on the
 669 media property. However, such threshold established on gas-brine-media and time
 670 factors together with associated geophysical and geochemical processes will serve a
 671 caution on the limit of sequestration for site-specific assessments.

672

673 **5. P^c -S- K_r relationships and phase characteristics in scCO₂-brine system**

674 Some properties of CO₂-water system had been discussed above and are shown to be
 675 temperature and pressure dependent. Among them, the interfacial tension of CO₂-water
 676 had been shown to decrease with increasing pressure and attains a plateau in the
 677 supercritical state (Espinoza and Santamarina 2010; Kvamme et al. 2007). In contrast,
 678 contact angle of the system also changes with pressure relative to the wettability of the
 679 medium. It increases with pressure on oil-wet surfaces and decreases slightly on water-
 680 wet surfaces (Chiquet et al. 2007; Espinoza et al. 2011). The implication of this
 681 behaviour on two-phase flow characteristics can be discerned based on Young-Laplace
 682 relation: $P^c = \frac{2\gamma^{wn} \cos \theta}{r}$ where P^c decreases with decrease in interfacial tension, γ^{wn} ,
 683 and increase in contact angle. Researchers of multiphase flow have reported patterns
 684 of $P^c - S - K_r$ relationship for multiphase flow and expatiated on number of factors
 685 affecting these relationships. Most of the works are published for oil-water system but of
 686 recent, we can find some studies relating to carbon sequestration. Changes in the
 687 interfacial tension as well as the contact angle will have impact on capillary pressure,
 688 residual saturation, evolution of flooding, capillary effects and relative permeabilities
 689 (Espinoza et al. 2011). Below, we examine the reports presented and the approaches
 690 adopted.



691

692 Figure 8: Density and viscosity of water and CO₂ with depth (Espinoza et al. 2011)

693

694 **5.1 Effects of viscosity and density ratios of CO₂ on P^c-S-K_r relationships**

695 The density and viscosity of the CO₂ have been shown to vary under different
696 conditions of pressure and temperature. In Figure 8, the density of CO₂ can be seen
697 following nonlinear rise from the surface to the injection bed about 1 km below ground
698 and then follow a fairly straight line into a deeper injection field about 3 km down for the
699 onshore sequestration. For the offshore operation this pattern changes as the density
700 rises rapidly around the sea bed and then remains almost constant henceforth and
701 larger at the same depth compared to onshore. In another part of the figure, the
702 viscosity of CO₂ in offshore and onshore follows similar though with slight variation in
703 values. On the other hand, the figure shows that the density of water remains constant
704 with depth while there is slight variation in its viscosity with depth. Implication of the
705 above properties behaviour is that at different depths of injection of CO₂ for
706 sequestration, the ratios of viscosity and density of CO₂ to that of brine will vary.
707 Viscosity and density ratios are some of the parameters identified to affect two-phase
708 flow in porous media (Das et al. 2007; Goel and O'Carroll 2011). In the context of
709 carbon sequestration, viscosity ratio refers to the ratio of the viscosity of non-wetting
710 phase i.e., scCO₂ (μ_{CO_2}) to that of the wetting phase i.e., water or brine (μ_w). This ratio

711 is mathematically expressed for viscosity as: $\mu_r = \frac{\mu_{CO_2}}{\mu_w}$ and density as: $\rho_r = \frac{\rho_{CO_2}}{\rho_w}$,

712 respectively. While discussing the rate dependency of the P^c – S – K_r relationships for
713 oil-water system, Joekar-Niasar and Hassanizadeh (2011) stated that the invading front
714 in a two-phase system becomes unstable if the viscosity ratio is less than one under
715 drainage or if greater than unity under imbibition while the front becomes stable if the
716 ratio is higher than one in drainage and lower than one in imbibition. This implies that
717 the displacement of brine by scCO₂ may face instability and the lower the viscosity ratio
718 at shallower depth, the higher the instability at the displacement front.

719

720 Das et al. (2007) pointed out that density ratio effect on P^c – S – K_r relationships is
721 dependent on the flow direction. The saturation-rate dependency of the relationships
722 also known as dynamic effect increases as density ratio increases if the flow is in
723 downward direction while the trend is still on the increase for decreasing density ratio if
724 the flow is in the upward direction (Das et al. 2006). Implication of the above discussion

725 in the characterisation of $P^c - S - K_r$ relationships for the $scCO_2$ -brine system in
726 different geological media will require applicable mathematical functions, which in no
727 doubt will be complex. Otherwise, the relationship will be determined for individual site.

728 729 **5.2 Instability in the displacement of fluid/fluid interface in $scCO_2$ -brine-porous** 730 **media system**

731 In a two-phase system in porous media, instability at the displacement front can occur
732 because of the higher mobility phase displacing a lower mobility phase as in the case of
733 $scCO_2$ -brine system leading to fingering of the displacing phase (Berg and Ott 2012).
734 This can be observed in both miscible and immiscible displacement conditions (Meurs
735 1957; Taylor 1958). Analytical model by Van Wunnik and Wit (1989) had earlier shown
736 the source of this condition to be as a result of viscous pressure gradient leading to a
737 steeper pressure gradient of the lower-mobility phase letting the finger grow. Among the
738 factors controlling this condition, mobility is defined as the ratio of the relative
739 permeability (K_r) of the phase to its viscosity (μ) and mobility ratio (m) as the ratio of the
740 mobility of the displacing phase to that of the displaced. For CO_2 displacing brine, m is
741 expressed in equation (15):

$$742$$
$$743 \quad m = \frac{K_{r_m} / \mu_n}{K_{r_w} / \mu_w}$$

744 (15)

745
746 K_{r_m} and μ_n are the relative permeability and viscosity of CO_2 , respectively while the K_{r_w}
747 and μ_w are the respective relative permeability and viscosity of water. It determines the
748 stability and the efficiency of the displacement (Berg and Ott 2012) which becomes
749 unstable at high m resulting in viscous fingering (Salimi et al. 2012). This is enhanced
750 by the much lower viscosity of the CO_2 .

751
752 Furthermore, capillarity was identified as another factor of importance affecting
753 instability growth rate (Yortsos and Hickernell 1989; Babchin et al. 2008) causing
754 'capillary dispersion' (Riaz and Tchelepi 2004) by which a sharp front becomes
755 transformed into a diffused zone with elongated tail (Berg and Ott 2012). This
756 dispersion effect acts to suppress finger (Homsy 1987). In addition, the scale of
757 consideration determines the influence of this capillarity as the dispersion occurs at the

758 same length scale as the shock front. Capillary number, Ca , is used to quantify the
759 influence of this force and it is defined as the ratio of the viscous to capillary forces
760 expressed as: $Ca = \mu V / \gamma$, μ is the viscosity of the displacing fluid, V the characteristic
761 velocity and γ is the interfacial tension between the two phases. Change in Ca has
762 been shown to affect the stability of the two-phase displacement patterns at different
763 values of m . Numerical simulations results by Lenormand et al. (1988) showed that at
764 high m and low Ca ($-8 < \text{Log } Ca < -6$), capillary fingering dominates the displacement
765 which becomes stable at high Ca (Figure 9a). At low m (Figure 9b), there exists a
766 crossover region as the Ca increases. At this region the displacement mechanisms
767 switches from the capillary to viscous fingering. Noticeable from the figure, at high m , is
768 the improved saturation of the displacing phase as the displacement transitioned to
769 stable displacement at appropriate Ca . Also, the figure showed the possibility of
770 inefficient storage that may result from operating under viscous fingering at low m .
771 Wang et al. (2013) demonstrated the influence of the Ca and the significance crossover
772 on the displacement of water by $scCO_2$. They found increase in $scCO_2$ saturation as the
773 $\text{log}Ca$ increases from -7.61 to -6.61 where capillary fingering dominates. At higher
774 injection rates, viscous fingering dominates, and the $scCO_2$ saturation remains nearly
775 constant.

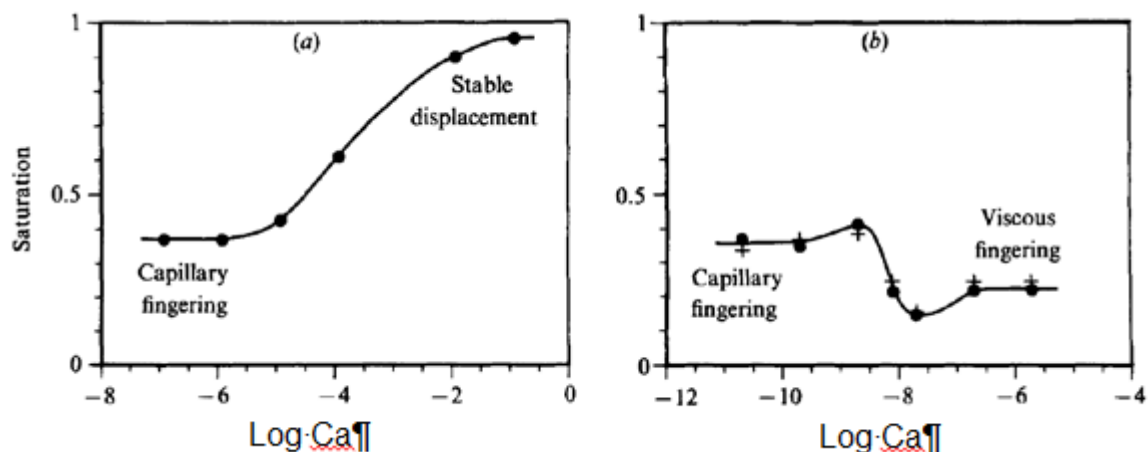
776
777 Furthermore, the Ca equation, shown above, indicates the importance of the interfacial
778 tension in the two-phase flow system. This also tells us some information about the
779 stability of the system. For example, in the numerical simulation by Berg and Ott (2012),
780 low interfacial tension in the range of $0-0.05$ mN/m generally leads to unstable
781 displacement while marginal stability is recorded at 0.1 mN/m. For interfacial energy
782 that is greater than 1 mN/m, it becomes stable at an experimental scale.

783
784 Various factors have been reported to affect the γ between CO_2 /water or CO_2 /brine
785 system. These include the temperature, pressure, salt concentrations and type of ions
786 in the system. Under similar conditions, γ for CO_2 /water and CO_2 /brine show similar
787 evolution with respect to temperature and temperature (Chun and Wilkinson 1995;
788 Chalbaud et al. 2010). It decreases with pressure at constant temperature and this is
789 more significant at lower pressure near the critical region (Nielsen et al. 2012; Shojai
790 Kaveh et al. 2011) especially at low temperature (Chalbaud et al. 2010). At higher
791 pressure, plateau is reached at the value of γ for the system that slight increases with

792 salt concentration at constant temperature (Chalbaud et al. 2010). This behaviour has
 793 been attributed to the solubility effects of CO₂ which increases with pressure at low
 794 pressure and remains nearly unchanged at higher pressure when the difference in
 795 densities between CO₂ and brine remains constant. Considering the dissolution effect
 796 on the density difference ($\Delta\rho$) become more important at high pressure since γ
 797 calculation is a linear function of $\Delta\rho$ (Chalbaud et al. 2010; Chiquet et al. 2007). For a
 798 given height of stored CO₂, underestimating the γ between CO₂/water will lead to
 799 overestimating the displacement efficiency making it seem like there is more space for
 800 storage than in reality (Chalbaud et al. 2010). The valence of the cations present in the
 801 gas-brine-rock system has been shown to be important in the value of the γ . For CO₂-
 802 water system, γ is more than twice higher for the divalent cation (e.g., Ca⁺²) than the
 803 monovalent type e.g., Na⁺ (Aggelopoulos et al. 2010).

804
 805 In addition, the viscosity ratio and the non-wetting phase saturation have relation to the
 806 Ca and the stability of the two-phase system. Zhang et al. (2011) observe higher
 807 incident of viscous fingers in the two-phase flow at high Ca. For very low viscosity ratio,
 808 unstable displacement dominates with the viscous fingers for all Ca. For moderately low
 809 viscosity ratio, there exists a value in Ca at which there is a crossover from unstable to
 810 stable displacement. This condition corresponds to $\log\mu_r > 0$ (Zhang et al. 2011). Based
 811 on Figure 8, at moderate depths of the aquifers (between 500 to 1000m), stable
 812 displacement is enhanced at offshore sites where CO₂ viscosity is higher.

813



814
 815 Figure 9: Capillary number and the displacement in the two-phase system (a) high
 816 viscosity ratio ($\log m = 1.9$), (b) low viscosity ratio ($\log m = -4.7$). Vertical axis
 817 represents the saturation of the displacing phase (Lenormand et al. 1988).

818

819 Authors like Plug and Bruining (2007) and Plug et al. (2006) acknowledge that the
820 supercritical CO₂ state is prone to phase transition together with property fluctuation.
821 These behaviours may not be unexpected to affect the stability and the $P^c - S - K_r$
822 relationships for the system. Plug and Bruining (2007) observed irregular P^c -S
823 relationships for supercritical CO₂ (at 40⁰C and 85 bar) under drainage while usual P^c -S
824 curve pattern was obtained for liquid CO₂ (27⁰C and 85 bar). This was attributed to
825 CO₂-wet behaviour or occasional imbibition of water during the process. This behaviour
826 can also be viewed as part of the manifestation of the above-described instability in the
827 displacement. scCO₂ phase undergoes irregular transition in properties and
828 characteristics at slight change of temperature, pressure and velocity which are difficult
829 to maintain constant in the system. The fact that this is absent in liquid case points to
830 the fact that reduced interfacial tension in scCO₂ (Nielsen et al. 2012; Espinoza and
831 Santamarina 2010) may be responsible judging from the report of Berg and Ott (2012).
832 Both authors (Nielsen et al. 2012; Espinoza and Santamarina 2010) reported that the
833 interfacial tension of CO₂-water system reduces with pressures but levels off above the
834 CO₂ critical condition (~7 MPa) at fixed temperature (Nielsen et al. 2012). However, the
835 work of Kaveh et al. (2013) show that the decrease continues up to 100 bar.
836 Furthermore, the sharp deviation in contact angle from the subcritical to supercritical
837 regions of CO₂ (Saraji et al. 2013) show that phase transition holds important
838 information about the phenomena in the scCO₂-brine system. Considering these cases,
839 phase transition in the geological media in conjunction with numerous subsurface
840 processes associated with scCO₂-brine and porous media systems may be complex
841 and point finger at the system stability and reliability.. This calls for more understanding
842 of the fluid-fluid-media system and characteristics, e.g., P^c -S- K_r relationships under the
843 varying conditions. K_r -S functions is essential for accurate analyses of the CO₂-water
844 displacement process (Berg and Ott 2012).

845

846 **5.3 Influence of pressure, dissolution and wettability**

847 The comparisons made between N₂ and CO₂ experiments by the Plug and Bruining
848 (2007) showed that CO₂ dissolution in water results in lower residual gas saturation.
849 This is similar to the findings of Pistone et al. (2011). Also, the capillary pressure of
850 scCO₂ was found to be lower if compared to gas and liquid CO₂ at every corresponding
851 saturation. Several authors (Tokunaga et al. 2013; Plug and Bruining 2007) are

852 unanimous in their observations that the $P^c - S$ relationships decrease as pressure
853 increases owing to decreasing interfacial tension (Chun and Wilkinson 1995; Espinoza
854 et al. 2011) while for secondary imbibition the negative P^c at around high water
855 saturation was attributed to alteration in wetting behaviour (Plug and Bruining 2007).
856 Though the effects of dissolution were more pronounced for the CO_2 injection
857 compared to N_2 , the capillary pressure was said not to be affected by the dissolution
858 since the P^c curves in both cases appear in the same range. But, it is well known that
859 the dissolution effects act to reduce the surface tension of a two-phase system as
860 earlier pointed out by Bennion and Bachu (2008) for CO_2 -brine and H_2S -brine systems.
861 Therefore, it is difficult to rule out the effect of dissolution on the observed differences in
862 $P^c - S$ at higher pressures. For $scCO_2$, small perturbations in the system dynamics
863 cause sudden events resulting in the spontaneous imbibition of water into the system
864 during drainage (Plug and Bruining 2007). This results in a decreasing capillary
865 pressure and an irregular drainage curve. Also, wettability effect showed that the sand
866 remains water-wet going by the positive drainage capillary pressure measured for all
867 temperature and pressure conditions considered. Plug et al. (2006) showed that coal
868 bed was water-wet in primary drainage but increasing pressure changes this to CO_2 -
869 wet condition in medium rank coal. They found that the effects of adsorption were not
870 very pronounced with the significant CO_2 -wet condition re-occurring for the imbibition
871 processes conducted. Their reports concluded that imbibition experiments provide good
872 qualitative information regarding the wettability of coal.

873

874 **5.4 $P^c - S - K_r$ relationships in consolidated porous rocks**

875 The work of Pini et al. (2012) reported $P^c - S$ for consolidated media, namely, the
876 Berea and Arqov sandstone samples. Discussing the relation in reference to
877 temperature, the $P^c - S$ curves for the Berea sandstone showed that capillary pressure
878 decreases as temperature reduces and this behaviour was attributed to increase in CO_2
879 dissolution as the temperature decreases reducing the interfacial tension. By
880 implication, the supercritical CO_2 will have a higher P^c than liquid CO_2 . But this will
881 contradict the conclusion of other authors that the liquid CO_2 has higher P^c than $scCO_2$
882 (Plug and Bruining 2007). Also, the $P^c - S$ profile in Berea sandstone, described as
883 well sorted and homogenous sample, was consistently low for wide range of saturation
884 with sharp rise in $P^c - S$ values close to irreducible saturation. In comparison, the
885 Arqov sample described as heterogeneous in nature displays a sharper rise and

886 broader distribution in $P^c - S$ while the profile remains considerably higher than in
887 Berea sandstone for most of the saturation values. This brings to mind the influence of
888 heterogeneities in $P^c - S$ relation as earlier reported for oil-water system (Mirzaei and
889 Das 2007) as the micro-heterogeneities are abundant in oil reservoirs (Van Lingen et al.
890 1996; Pickup et al. 2005). A list of experimental methods, fluid and media
891 characteristics and various equipment applications by various authors in connection
892 with $P^c - S - K_r$ determination for scCO₂-brine system in the context of geological
893 sequestration is shown in Table 2.

894

895 **6.0 Leakage risks and monitoring**

896 Risks of leakage of stored carbon dioxide portend serious dangers to the potable water
897 aquifers that may lie along the escape paths. Also, on the earth's surface, living species
898 are susceptible to CO₂ inhalation while leakage through the ocean with consequent
899 acidification poses harm to marine life. Technically, leaks could occur as results of
900 gravity override together with viscous instability causing the carbon dioxide to move to
901 the top of the injection layer bypassing large quantities of brine (Gasda 2008; Saripalli
902 et al. 2001; Metz et al. 2005). If the caprock however has favourable pathways, the
903 carbon dioxide could escape vertically compromising the intention of the process. The
904 vertical buoyant pressure applied on the caprock by the carbon dioxide is as a result of
905 difference in density between the formation waters and the carbon dioxide, and the
906 thickness of the carbon dioxide plume accumulation.

907

908 Monitoring technologies are widely discussed in the literature. They are built upon the
909 physico-chemical properties of the CO₂-brine-rock system or the detection of the
910 reaction by-products or even the coupled process effects such as micro-seismicity
911 (Espinoza et al. 2011). Methods like electrical resistivity and wave propagation are most
912 often employed in deep reservoir applications (Nakatsuka et al. 2010) while application
913 of tracers like SF₆ aid the monitoring of fluid movement. The monitoring methods
914 should extend several hundred meters beyond the injection region to safely check the
915 advancing plume of CO₂. In addition, monitoring the deep region around the aquifers
916 should be coupled with near surface and surface monitoring.

917

918 To this end, available technologies should be adequately utilised. These include:
919 electromagnetic techniques (Nakatsuka et al. 2010), temperature signals (Bielinski et al.

920 2008) and infrared monitoring (Charpentier et al. 2009) that have been demonstrated
921 either in the laboratory or pilot applications for subsurface monitoring. Methods like
922 electromagnetic techniques utilise the wide gap between the dielectric permittivities of
923 CO₂ and water to create contrast with reference the CO₂ saturation in the domain. Non-
924 isothermal effects such as CO₂ dissolution and change of phase are made use of in the
925 temperature signal method while the characteristic infrared wave absorption property of
926 CO₂ is harnessed in the infrared monitoring technique. Near surface monitoring is also
927 essential as stated before and this involves the analysis of near surface water, air and
928 soil samples on a regular basis as CO₂ leaks can acidify the water and create
929 conspicuous contrast between the original and current soil and air compositions. On the
930 surface, the use of gravity method (Alnes et al. 2008) as CO₂ is heavier than air and
931 lighter than water, remote sensing of air composition (Leuning et al. 2008) and surface
932 analysis of carbon content by Inelastic Neutron Scattering (INS) (Wielopolski and Mitra
933 2010) have been reported. Overall, monitoring protocols are essential for effectiveness
934 of success of geological sequestration of CO₂.

935

936 **7.0 Concluding remarks**

937 To address the issues of climate change and the problems of global warming requires
938 meticulous scientific and engineering approaches. The current opinions favour
939 geological sequestration option. Therefore, scCO₂-brine-rock interactions together with
940 the *in situ* processes and trapping mechanisms should be quantified accurately as they
941 play significant roles in determining the efficiency and safety of these processes. . Out
942 of many candidate sites, choosing an appropriate geological site requires optimizing the
943 process functions relating to the media, fluid and operational characteristics. This is
944 more so as these characteristics directly or indirectly affect the processes which
945 determine safe CO₂ storage, e.g., dissolution and structural trapping, reaction and
946 mineral precipitation, etc. CO₂ solubility is influenced by the porosity and pore size
947 distribution (Emmanuel et al. 2010). So, developing the optimization protocols will aid
948 the general practices in this regard. In relation to this, mathematical modelling and
949 simulation tools have played significant roles, providing insightful predictions of the fate
950 of the stored carbon and various processes including the trapping mechanisms. But,
951 the site-specific indicators of CO₂ leakage, and predictable compromise of reservoir
952 integrity with the quantity and dynamics of CO₂ in the reservoir are desired to be
953 integrated in the system software with fully-coupled geochemical, fluid-fluid-solid,
954 hydrogeological, physical and chemo-physical conditions. Such indicator or factor

955 should consider the impact of man-made leakage zone (see, e.g., (Humez et al. 2011;
956 Tao and Bryant 2014)) as well as natural-leakage zone (see, e.g., (Schwartz 2014)).
957 Affordable and commercial availability of the software products will drive research and
958 field developments.

959
960 As a special kind of two-phase flow system, $P^c - S - K_r$ relationships for scCO₂-brine-
961 rock system are important in the modelling and analysis of the sequestration operations.
962 But, the list of available experimental publications is far from sufficient especially when
963 viewed from possible factors that can affect $P^c - S - K_r$ relationships from closely
964 related process as encountered in the studies of oil recovery, oil spill remediation,
965 contaminant transport and so on. Wettability of the medium is shown to be responsible
966 for the irregularity in the pattern of $P^c - S - K_r$ relationships (Plug and Bruining 2007)
967 with the possibility of *in situ* alteration in media wettability. This needs further
968 investigation in order to keep the function applicable in the modelling and prediction of
969 sequestration process and storage safety.

970
971 Most of the $P^c - S - K_r$ relationships reported are related to quasi-static or equilibrium
972 conditions. The dynamic behaviour of the system particularly at the immediate time
973 following injection prior to the attainment of equilibrium needs to be better understood.
974 In this regards, the difference in the quasi static or dynamically measured $P^c - S - K_r$
975 relationships will be of interests. Researchers of multiphase flow had dedicated past
976 decades to the study of various dynamic effects in system properties of multiphase flow.
977 Part of the investigations dwelled largely on the saturation-rate dependency of the
978 system properties and a number of publications had resulted (Hassanizadeh and Gray
979 1993; Das et al. 2007; Mirzaei and Das 2007; Hanspal and Das 2012; Dahle et al. 2005;
980 Goel and O'Carroll 2011; Das and Mirzaei 2013). Particularly for $P^c - S$ relationships,
981 the dynamic coefficient, τ , used in quantifying this phenomenon has been said to be
982 dependent on media permeability (Mirzaei and Das 2007; Tian et al. 2012; Hanspal and
983 Das 2012; Dahle et al. 2005), microheterogeneity (Mirzaei and Das 2007), fluid
984 properties (Das et al. 2007; Goel and O'Carroll 2011), scale of observation (Dahle et al.
985 2005; Bottero et al. 2006 ; Bottero et al. 2011; Nordbotten et al. 2007), etc. Though, the
986 observations and reports were made largely in relation to oil-water system, investigating
987 the same effects for the rock-scCO₂-brine system will broaden the present state of

988 study while improving the applicability and integrity of $P^c - S - K_r$ relationships as a
989 modelling function for the rock-scCO₂-brine system.

990
991 For example, different media permeabilities are encountered and hardly can two porous
992 media share the same permeability even at a contiguous sediment. A look at Table 2
993 reveals this reality as each experiment has different media permeability unique to it.
994 Even within an aquifer or reservoir, media anisotropy may be assumed but the reality
995 dictates otherwise (Pickup et al. 2005; Nordbotten et al. 2007; Aggelopoulos and
996 Tsakiroglou 2008). Micro-heterogeneities are another closely related property of the
997 porous media. These are abundant in the reservoir (Van Lingen et al. 1996; Pickup et al.
998 2005) and they affect the micro and macro scale quantity of the system variables while
999 τ is said to increase with its intensity (Mirzaei and Das 2007). Aquifer or reservoir
1000 exhibits these properties or characteristics with few exceptions and are worth
1001 investigating in the context of carbon sequestration, especially the way they affect the
1002 $P^c - S - K_r$ relationships.

1003
1004 To determine $P^c - S$ relationships for two-phase flow in any aquifer or reservoir,
1005 pressures in both phases need to be measured separately and saturation
1006 simultaneously determined. From the literature discussed in this review, it seems that
1007 the common laboratory measurement methods used for determining the $P^c - S$
1008 parameters for scCO₂-brine/water system can be better described as pressure drop
1009 across the domain to get the P^c and the measurement of the outflow water or brine for
1010 the saturation. An advanced *in situ* saturation measurement method was presented by
1011 Pini et al. (2012) using a medical X-ray CT scanning instrument with good resolution.
1012 This has the additional ability to determine the sample porosity. But the cost of this
1013 instrument and technicalities may pose challenges to many promising investigations. To
1014 overcome this, instruments like time domain reflectometer (TDR) can be recommended.
1015 They had been variously used to obtain *in situ* saturation measurement for decades
1016 (Das and Mirzaei 2013; Goel and O'Carroll 2011; Camps-Roach et al. 2010; Topp et al.
1017 1984). Most of these experiments were conducted for oil-water and air-water systems
1018 mostly at near ambient condition but the instrument is still easily adaptable to the
1019 supercritical condition of carbon sequestration. The TDR probe has the capacity to
1020 determine the bulk electrical conductivity of the system in addition to the dielectric
1021 constant used in determining water saturation.

1022 **Table 2:** Typical P^c-S-K_r experiments for scCO₂-brine/water system in the literature (D: diameter L: Length)

Author(s)	Porous Materials	Fluid	Permeability (m ²)	Porosity	Process Condition(s)	Equipment Type	P ^c Measurement Method	Sample Dimensions (cm)
Plug and Bruining (2007)	Unconsolidated sand	scCO ₂ - water	2 x 10 ⁻¹⁰	0.36	21-40 (°C), 1-85 (bar)	Porous plate and micropore technique	Pressure difference across domain	8.4 (D) 2.5 (L)
Plug et al. (2006)	Unconsolidated sand, coal		—	0.36-0.38 (sand), 0.42-0.45 (coal)	21-40 (°C), 1-85 (bar)	Porous plate and micropore technique	Pressure difference across domain	8.4 (D) 2.5 (L)
Tokunaga et al. (2013)	Unconsolidated sand		3.9 x 10 ⁻¹¹	0.381	45 (°C) 85-120 (bar)	Porous plate	Externally controlled fluid-fluid interface adjustment in relation to reference plane	8.2 (D) 3 (L)
Pentland et al. (2011)	Consolidated sandstone	scCO ₂ - brine	4.6 x 10 ⁻¹³	0.22	70 (°C) 90 (bar)	Porous plate	Pressure difference across domain	3.85 (D) 7.53 (L)

Pini et al. (2012)			2.7×10^{-13}	19.5	25-50 (°C) 90 (bar)	Modified porous plate		5 (D) 9 (L)
-----------------------	--	--	-----------------------	------	------------------------	--------------------------	--	----------------

1023

1024 It has been argued that external measurement of capillary pressure loses
1025 significance near residual saturation (Morrow and Harris 1965; Bottero 2009) as the
1026 non-wetting phase pressure dominates at this period when the wetting phase
1027 experience disconnectivity and thus making the measured wetting phase pressure
1028 appear larger. This makes the P^c smaller than supposed. But, the challenges of *in*
1029 *situ* phase pressure measurement are not simple, considering the high pressure and
1030 above ambient temperature of the supercritical CO₂. At this state, most of the semi
1031 permeable membranes used by many authors (Das and Mirzaei 2012; Bottero et al.
1032 2011; Hou et al. 2012) or porous ceramic discs (Camps-Roach et al. 2010; Goel and
1033 O'Carroll 2011) employed in oil-water or air-water systems will fail to distinguish any
1034 phase under supercritical condition as they were designed to operate under ambient
1035 conditions. However, there is hope in some of the metallic materials recently used by
1036 some authors under similar conditions even though they were not used to measure
1037 phase pressures. For example, C276 Hastelloy porous plate used by Tokunaga et al.
1038 (2013) and aluminium silicate by Pentland (2011) were described as semi permeable
1039 hydrophobic and hydrophilic discs, respectively under the supercritical conditions.
1040 Many other materials may still be available from membrane manufacturers to
1041 achieve this aim.

1042

1043 The effect of scale on dynamic effect in $P^c - S - K_r$ relationships is also well reported
1044 (Dahle et al. 2005; Bottero et al. 2011; Camps-Roach et al. 2010). Most of the
1045 experiments available for scCO₂-brine-rock system are, at most, at the core scale
1046 size. How these relationships vary with size of the aquifer or field scale will be of
1047 great importance in the complete assessment of the factors affecting the $P^c - S - K_r$
1048 functions and will improve the versatility of their applications. The following bullet
1049 points will help to emphasis some suggestions based on this review:

1050

- 1051 • There are needs for experimental investigations of the effects of media
1052 characteristics e.g., domain scale, on the $P^c - S - K_r$ relationships for scCO₂-
1053 brine system at conditions applicable to geological carbon sequestration.
- 1054 • To promote our understanding of caprock integrity, investigations of the pore
1055 size distribution on relative permeability of CO₂ needs to be made clearer in

1056 conjunction with interfacial tension of the scCO₂-brine system. For example,
1057 one may ask, 'how does the combination affect the entry pressure of the
1058 caprock?' Such investigations need to be conducted in the context of pressure,
1059 temperature, salt concentration, cation valence that are known to influence
1060 the interfacial tension. Contributions of the long-time mineral precipitation to
1061 change in salinity, combinations of cation valences and their effects on the
1062 above parameters will be very enlightening.

- 1063 • Use of surfactants to curtail migration of scCO₂ in saline aquifer and promote
1064 residual trapping will deserve future investigations, e.g., can surfactants check
1065 viscous and capillary fingerings in scCO₂-brine-rock systems? There are
1066 many works on the use of surfactant and CO₂ in literature which are related to
1067 enhanced oil recovery (EOR).
- 1068 • Inclusion of leakage parameters on a site-specific basis in the modelling and
1069 simulation of the system should be encouraged.
- 1070 • The dynamic capillary pressure effects for the $P^c - S - K_r$ relationships should
1071 be investigated in relation to scCO₂-brine-rock system and these relationships
1072 should be incorporated in the relevant simulators for the geological carbon
1073 sequestration.
- 1074 • The wettability alteration and the caprock integrity from the perspective of the
1075 alternation of the scCO₂-brine-rock system conditions from neutrality to acidity
1076 and alkalinity as a result chemical complexation and mineral dissolution
1077 deserve more investigations. As different cationic valences change the
1078 interfacial tensions, how do similar changes in the subsurface conditions
1079 affect the wettability? This will be an important question to answer in future
1080 investigations.
- 1081 • How continuous or intermittent injection and its rates influence residual
1082 trapping of injected CO₂ will be a subject of interesting investigations.
- 1083 • Cheap and simple CO₂ leakage detection system should be developed for
1084 common household to be used for the independent assessment of CO₂ gas
1085 accumulation, especially for residents closer to transport pipeline or geo-
1086 sequestration sites.

1087

1088 **References**

- 1089 Abu-Khader, M.M., 2006. Recent Progress in CO₂ Capture/Sequestration: A Review.
1090 *Energy Sources, Part A: Recovery, Utilization, and Environmental Effects*,
1091 28(14), pp.1261–1279.
- 1092 Aggelopoulos, C. A., Robin, M., Perfetti, E. and Vizika, O., 2010. CO₂/CaCl₂ solution
1093 interfacial tensions under CO₂ geological storage conditions: Influence of cation
1094 valence on interfacial tension. *Advances in Water Resources*, 33(6), pp.691–
1095 697.
- 1096 Aggelopoulos, C. A. and Tsakiroglou, C.D., 2008. The effect of micro-heterogeneity
1097 and capillary number on capillary pressure and relative permeability curves of
1098 soils. *Geoderma*, 148(1), pp.25–34.
- 1099 Alabi, O.O., 2011. Fluid Flow in Homogeneous and Heterogeneous Porous Media.
1100 *Electronic Journal of Geotechnical Engineering*, 16.
- 1101 Algive, L., Bekri, S., Vizika-kavvadias, O., 2009. Reactive pore network modeling
1102 dedicated to the determination of the petrophysical property changes while
1103 injecting CO₂. In *SPE Annual Technical conference and Exhibition*.
- 1104 Alnes, H., Eiken, O. and Stenvold, T., 2008. Monitoring gas production and CO₂
1105 injection at the Sleipner field using time-lapse gravimetry. *Geophysics*, 73(6),
1106 pp.WA155–WA161.
- 1107 Anderson, W., 1987. Wettability Literature Survey Part 5: The Effects Of Wettability
1108 On Relative Permeability. *Journal of Petroleum Technology*, 39(11), pp.1453–
1109 1468.
- 1110 Babchin, A., Brailovsky, I., Gordon, P. and Sivashinsky, G., 2008. Fingering
1111 instability in immiscible displacement. *Physical Review-Series E*, 77(2), 026301.
- 1112 Bear, J., 2013. *Dynamics of fluids in porous media*, Courier Dover Publications.

- 1113 Beni, A.N., Kühn, M., Meyer, R. and Clauser, C., 2012. Numerical modeling of a
1114 potential geological CO₂ sequestration site at Minden (Germany). *Environmental*
1115 *Modeling & Assessment*, 17(4), pp.337–351.
- 1116 Bennion, B. and Bachu, S., 2008. and imbibition relative permeability relationships
1117 for supercritical CO₂/brine and H₂S/brine systems in intergranular sandstone,
1118 carbonate, shale, and anhydrite rocks. *SPE Reservoir Evaluation & Engineering*,
1119 11(3).
- 1120 Benson, S.M. and Cole, D.R., 2008. CO₂ sequestration in deep sedimentary
1121 formations. *Elements*, 4(5), pp.325–331.
- 1122 Bentham, M., 2006. An assessment of carbon sequestration potential in the UK--
1123 Southern North Sea case study. *Tyndall Centre for Climate Change Research*
1124 *and British Geological Survey. Keyworth, Nottingham, UK: Kingsley Dunham*
1125 *Centre*.
- 1126 Berg, S. and Ott, H., 2012. Stability of CO₂-brine immiscible displacement.
1127 *International Journal of Greenhouse Gas Control*, 11, pp.188–203.
- 1128 Bickle, M., Chadwick, A., Huppert, H. E., Hallworth, M. and Lyle, S., 2007. Modelling
1129 carbon dioxide accumulation at Sleipner: Implications for underground carbon
1130 storage. *Earth and Planetary Science Letters*, 255(1), pp.164–176.
- 1131 Bielinski, A., Kopp, A., Schütt, H. and Class, H., 2008. Monitoring of CO₂ plumes
1132 during storage in geological formations using temperature signals: Numerical
1133 investigation. *International Journal of Greenhouse Gas Control*, 2(3), pp.319–
1134 328.
- 1135 Bissell, RC, Vasco DW, Atbi M, Hamdani M, Okwelegbe M, Goldwater MH., 2011. A
1136 full field simulation of the in Salah gas production and CO₂ storage project using
1137 a coupled geo-mechanical and thermal fluid flow simulator. *Energy Procedia*, 4,
1138 pp.3290–3297.
- 1139 Bottero, S., Hassanizadeh, S. M., Kleingeld, P. J. and Bezuijen, A., 2006.
1140 Experimental study of dynamic capillary pressure effect in two-phase flow in

- 1141 porous media. In *Proceedings of the XVI International Conference on*
1142 *Computational Methods in Water Resources (CMWR), Copenhagen, Denmark*
1143 (pp. 18-22).
- 1144 Bottero, S., Hassanizadeh, S. M., Kleingeld, P. J., and Heimovaara, T. J., 2011.
1145 Nonequilibrium capillarity effects in two-phase flow through porous media at
1146 different scales. *Water Resources Research*, 47(10).
- 1147 Bottero, S., 2009. *Advances in the Theory of Capillarity in Porous Media*. Universiteit
1148 Utrecht.
- 1149 Bottero, S., Hassanizadeh, S. M. and Kleingeld, P. J., 2011. From Local
1150 Measurements to an Upscaled Capillary Pressure–Saturation Curve. *Transport*
1151 *in Porous Media*, 88(2), pp.271–291.
- 1152 Bower, K.M. and Zyvoloski, G., 1997. A numerical model for thermo-hydro-
1153 mechanical coupling in fractured rock. *International Journal of Rock Mechanics*
1154 *and Mining Sciences*, 34(8), pp.1201–1211.
- 1155 Brooks, R. and Corey, A., 1964. Hydraulic Properties of Porous Media. *Hydrology*
1156 *Papers. Colorado State University*.
- 1157 Burdine, N., 1953. Relative permeability calculations from pore size distribution data.
1158 *Journal of Petroleum Technology*, 5(03), pp.71–78.
- 1159 Burdine, N.T., Gournay, L.S. and Reichertz, P.P., 1950. No Title“Pore Size
1160 Distribution of Petroleum Reservoir Rocks.” *Trans. AIME*, 198, pp.195–204.
- 1161 Camps-Roach, G., O’Carroll, D. M., Newson, T. A., Sakaki, T. and Illangasekare, T.
1162 H., 2010. Experimental investigation of dynamic effects in capillary pressure:
1163 Grain size dependency and upscaling. *Water Resources Research*, 46(8).
- 1164 Chadwick, A., Arts, R., Bernstone, C. and May, F., 2008. *Best Practice for the*
1165 *Storage of CO₂ in Saline Aquifers-Observations and Guidelines from the SACS*
1166 *and CO2STORE projects*,

- 1167 Chalbaud, C., Robin, M., Lombard, J., Bertin, H. and Egermann, P., 2010. Brine / CO
1168 2 Interfacial Properties and Effects on CO₂ Storage in Deep Saline Aquifers.
1169 65(4), pp.541–555.
- 1170 Chang, Y.-B., Coats, B. and Nolen, J., 1998. A Compositional Model for CO₂ Floods
1171 Including CO₂ Solubility in Water. *SPE Reservoir Evaluation & Engineering*, 1(2),
1172 pp.155–160.
- 1173 Charpentier, F. et al., 2009. Infrared monitoring of underground CO₂ storage using
1174 chalcogenide glass fibers. *Optical Materials*, 31(3), pp.496–500.
- 1175 Chiquet, P., Broseta, D. and Thibeau, S., 2007. Wettability alteration of caprock
1176 minerals by carbon dioxide. *Geofluids*, 7(2), pp.112–122.
- 1177 Chun, B.-S. and Wilkinson, G.T., 1995. Interfacial tension in high-pressure carbon
1178 dioxide mixtures. *Industrial & Engineering Chemistry Research*, 34(12),
1179 pp.4371–4377.
- 1180 Class, H., Ebigbo, A., Helmig, R., Dahle, H. K., Nordbotten, J. M., Celia, M. A., and
1181 Wei, L., 2009. A benchmark study on problems related to CO₂ storage in
1182 geologic formations. *Computational Geosciences*, 13(4), pp.409–434.
- 1183 Dahle, Helge K., Celia, M. a. and Majid Hassanizadeh, S., 2005. Bundle-of-Tubes
1184 Model for Calculating Dynamic Effects in the Capillary-Pressure- Saturation
1185 Relationship. *Transport in Porous Media*, 58(1-2), pp.5–22.
- 1186 Das, DB. SM Hassanizadeh, BE Rotter, B Ataie-Ashtiani (2004). A numerical study
1187 of micro-heterogeneity effects on upscaled properties of two-phase flow in
1188 porous media. *Transport in porous media* 56 (3), 329-350
- 1189 Das, D.B., Gaudie, R. and Mirzaei, M., 2007. Dynamic Effects for Two-Phase Flow
1190 in Porous Media : Fluid Property Effects. *AIChE* , 53(10), pp. 2505-2520.
- 1191 Das, D.B. and Mirzaei, M., 2012. Dynamic effects in capillary pressure relationships
1192 for two-phase flow in porous media: Experiments and numerical analyses.
1193 *AIChE Journal*, 58(12), pp.3891–3903.

- 1194 Das, D.B. and Mirzaei, M., 2013. Experimental measurement of dynamic effect in
1195 capillary pressure relationship for two-phase flow in weakly layered porous
1196 media. *AIChE Journal*, 59(5), pp.1723–1734.
- 1197 Das, D.B., Mirzaei, M. and Widdows, N., 2006. Non-uniqueness in capillary
1198 pressure–saturation–relative permeability relationships for two-phase flow in
1199 porous media: Interplay between intensity and distribution of random micro-
1200 heterogeneities. *Chemical Engineering Science*, 61(20), pp.6786–6803.
- 1201 Dodds, W.S., Stutzman, L.F. and Sollami, B.J., 1956. Carbon dioxide solubility in
1202 water. *Chemical & Engineering Data Series*, 1(1), pp.92–95.
- 1203 DOE, 2010. Fossil. Available at: [http://www.energy.gov/science-innovation/energy-](http://www.energy.gov/science-innovation/energy-sources/fossil)
1204 [sources/fossil](http://www.energy.gov/science-innovation/energy-sources/fossil).
- 1205 Dollimore, D. and Heal, G.R., 1964. An improved method for the calculation of pore
1206 size distribution from adsorption data. *Journal of Applied Chemistry*, 14(3),
1207 pp.109–114.
- 1208 Doughty, C., 2007. Modeling geologic storage of carbon dioxide: Comparison of non-
1209 hysteretic and hysteretic characteristic curves. *Energy Conversion and*
1210 *Management*, 48(6), pp.1768–1781.
- 1211 Drever, J.I. and Stillings, L.L., 1997. The role of organic acids in mineral weathering.
1212 *Colloids and Surfaces A: Physicochemical and Engineering Aspects*, 120(1),
1213 pp.167–181.
- 1214 Duan, Z. and Sun, R., 2003. An improved model calculating CO₂ solubility in pure
1215 water and aqueous NaCl solutions from 273 to 533 K and from 0 to 2000 bar.
1216 *Chemical Geology*, 193(3), pp.257–271.
- 1217 Emmanuel, S., Ague, J.J. and Walderhaug, O., 2010. Interfacial energy effects and
1218 the evolution of pore size distributions during quartz precipitation in sandstone.
1219 *Geochimica et Cosmochimica Acta*, 74(12), pp.3539–3552.

- 1220 Espinoza, D. N., Kim, S.H. and Santamarina, J. C., 2011. CO₂ geological storage —
1221 Geotechnical implications. *KSCE Journal of Civil Engineering*, 15(4), pp.707–
1222 719.
- 1223 Espinoza, D. Nicolas and Santamarina, J. Carlos, 2010. Water-CO₂ -mineral
1224 systems: Interfacial tension, contact angle, and diffusion-Implications to CO₂
1225 geological storage. *Water Resources Research*, 46(7).
- 1226 Farajzadeh, R., 2009. *Enhanced transport phenomena in CO₂ sequestration and*
1227 *CO₂ EOR*, PhD thesis, Technical University Delft, The Netherlands.
- 1228 Fleury, M. et al., 2010. Petrophysical measurements for CO₂ storage: application to
1229 the Ketzin site. *The Society of Core Analysts, SCA News SCA2010-06*, 22,
1230 pp.1–12.
- 1231 Fujii, T., Gautier, S, Gland, N., Boulin, P., Norden, B., Schmidt-Hattenberger, C.,
1232 2010. Sorption Characteristics of CO₂ on Rocks and Minerals in Storing CO₂
1233 Processes. *Natural Resources (2158-706X)*, 1(1).
- 1234 Garcia, J.E., 2001. Density of aqueous solutions of CO₂. Available at:
1235 <http://escholarship.org/uc/item/6dn022hb>.
- 1236 Gasda, S.E., 2008. *Numerical Models for Evaluating CO₂ Storage in Deep , Saline*
1237 *Aquifers: Leaky Wells and Large-Scale Geological Features* . Princeton
1238 University.
- 1239 Gaus, I., Azaroual, M. and Czernichowski-Lauriol, I., 2005. Reactive transport
1240 modelling of the impact of CO₂ injection on the clayey cap rock at Sleipner
1241 (North Sea). *Chemical Geology*, 217(3), pp.319–337.
- 1242 Goel, G. and O'Carroll, D.M., 2011. Experimental investigation of nonequilibrium
1243 capillarity effects: Fluid viscosity effects. *Water Resources Research*, 47(9).
- 1244 Gunter, W.D. et al., 2009. Heartland Area Redwater reef saline aquifer CO₂ storage
1245 project. *Energy Procedia*, 1(1), pp.3943–3950.

- 1246 Hansen, J. et al., 2008. Target atmospheric CO₂: Where should humanity aim? *arXiv*
1247 *preprint arXiv:0804.1126*.
- 1248 Hanspal, N. and Das, D., 2012. Dynamic effects on capillary pressure–saturation
1249 relationships for two-phase porous flow: Implications of temperature. *AICHE*
1250 *Journal*, 00(0), pp.1–15.
- 1251 Hassanizadeh, S Majid and Gray, W.G., 1993. Thermodynamic basis of capillary
1252 pressure in porous media. *Water Resources Research*, 29(10), pp.3389–3405.
- 1253 Homsy, G.M., 1987. Viscous fingering in porous media. *Annual Review of Fluid*
1254 *Mechanics*, 19(1), pp.271–311.
- 1255 Hou, L., Chen, L., Kibbey, T. C. G. and Street, W. B., 2012. Dynamic capillary effects
1256 in a small-volume unsaturated porous medium : Implications of sensor response
1257 and gas pressure gradients for understanding system dependencies, *Water*
1258 *Resources Research*, 48(11).
- 1259 Houghton, J.T., Ding, Y.D.J.G., Griggs, D. J., Noguier, M., van der LINDEN, P. J., Dai,
1260 X., Maskell, K., and Johnson, C. A., 2001. *Climate change 2001: the scientific*
1261 *basis*, Cambridge university press Cambridge.
- 1262 Huh, C., Kang, S. G., Hong, S., Choi, J. S., Baek, J. H., Lee, C. S., and Lee, J. S.,
1263 2009. CO₂ storage in marine geological structure: A review of latest progress
1264 and its application in Korea. *Energy Procedia*, 1(1), pp.3993–4000.
- 1265 Humez, P., Audigane, P., Lions, J., Chiaberge, C., and Bellenfant, G., 2011.
1266 Modeling of CO₂ leakage up through an abandoned well from deep saline
1267 aquifer to shallow fresh groundwaters. *Transport in porous media*, 90(1),
1268 pp.153–181.
- 1269 Huo, D. and Gong, B., 2010. Discrete Modeling and Simulation on Potential Leakage
1270 through Fractures in CO₂ Sequestration. In *SPE Annual Technical Conference*
1271 *and Exhibition*.

- 1272 Joekar-Niasar, V. and Majid Hassanizadeh, S., 2011. Effect of fluids properties on
1273 non-equilibrium capillarity effects: Dynamic pore-network modeling. *International*
1274 *Journal of Multiphase Flow*, 37(2), pp.198–214.
- 1275 Juanes, R., Spiteri, E. J., Orr, F. M. and Blunt, M. J., 2006. Impact of relative
1276 permeability hysteresis on geological CO₂ storage. *Water Resources Research*,
1277 42(12).
- 1278 Karl, T.R., Melillo, J.M. and Peterson, T.C., 2009. *Global climate change impacts in*
1279 *the United States*, Cambridge University Press.
- 1280 Khudaida, K and Das, DB (2014). A numerical study of capillary pressure - saturation
1281 relationship for supercritical carbon dioxide (CO₂) injection in deep saline
1282 aquifer. *Chemical Engineering Research and Design*, DOI:
1283 10.1016/j.cherd.2014.04.020 (in press).
- 1284 Kopp, A, Class, H and Helmig, R, 2009. Investigations on CO₂ storage capacity in
1285 saline aquifers: Part 1. Dimensional analysis of flow processes and reservoir
1286 characteristics. *International Journal of Greenhouse Gas Control*, 3(3), pp.263–
1287 276.
- 1288 Kvamme, B., Kuznetsova, T., Hebach, A., Oberhof, A., and Lunde, E., 2007.
1289 Measurements and modelling of interfacial tension for water+carbon dioxide
1290 systems at elevated pressures. *Computational Materials Science*, 38(3),
1291 pp.506–513.
- 1292 Lenormand, R., Delaplace, P. and Schmitz, P., 1998. Can we really measure the
1293 relative permeabilities using the micropore membrane method? *Journal of*
1294 *Petroleum Science and Engineering*, 19(1-2), pp.93–102.
- 1295 Lenormand, R., Touboul, E. and Zarcone, C., 1988. Numerical models and
1296 experiments on immiscible displacements in porous media. *J. Fluid Mech.*
1297 (1988),, 189(C), pp.165–187.

- 1298 Leuning, R., Etheridge, D., Luhar, A. and Dunse, B., 2008. Atmospheric monitoring
1299 and verification technologies for CO₂ geosequestration. *International Journal of*
1300 *Greenhouse Gas Control*, 2(3), pp.401–414.
- 1301 Li, L., Peters, C.A. and Celia, M.A., 2006. Upscaling geochemical reaction rates
1302 using pore-scale network modeling. *Advances in water resources*, 29(9),
1303 pp.1351–1370.
- 1304 Van Lingen, P., Bruining, J. and C.P.J.W., V., 1996. Capillary Entrapment Caused by
1305 Small-Scale Wettability Heterogeneities. *SPE Reservoir Engineering*, 11(2),
1306 pp.93–100.
- 1307 Marland, G. and Rotty, R.M., 1984. Carbon dioxide emissions from fossil fuels: A
1308 procedure for estimation and results for 1950--1982. *Tellus B*, 36(4), pp.232–
1309 261.
- 1310 Metz, B., Davidson, O., de Coninck, H., Loos, M., and Meyer, L., 2005. *IPCC special*
1311 *report on carbon dioxide capture and storage*, Intergovernmental Panel on
1312 Climate Change, Geneva (Switzerland). Working Group III. Cambridge
1313 University Press.
- 1314 Van Meurs, P., 1957. The use of transparent three-dimensional models for studying
1315 the mechanism of flow processes in oil reservoirs. In: *SPE Annual Technical*
1316 *Conference and Exhibition*, Anaheim, CA, vol. 210, pp. 295–301
- 1317 Michael, K., Golab, A., Shulakova, V., Ennis-King, J., Allinson, G., Sharma, S., and
1318 Aiken, T., 2010. Geological storage of CO₂ in saline aquifers—A review of the
1319 experience from existing storage operations. *International Journal of*
1320 *Greenhouse Gas Control*, 4(4), pp.659–667.
- 1321 Mirzaei, M. and Das, D.B., 2007. Dynamic effects in capillary pressure–saturations
1322 relationships for two-phase flow in 3D porous media: Implications of micro-
1323 heterogeneities. *Chemical Engineering Science*, 62(7), pp.1927–1947.

- 1324 Mirzaei, M and Das, DB (2013). Experimental investigation of hysteretic dynamic
1325 effect in capillary pressure–saturation relationship for two-phase flow in porous
1326 media. *AIChE Journal*, 59(10), 3958-3974.
- 1327 Morris, J. P., Hao, Y., Foxall, W. and McNab, W., 2011. In salah CO₂ storage JIP:
1328 hydromechanical simulations of surface uplift due to CO₂ injection at in salah.
1329 *Energy Procedia*, 4, pp.3269–3275.
- 1330 Morris, J. P., Detwiler, R. L., Friedmann, S. J., Vorobiev, O. Y. and Hao, Y., 2011.
1331 The large-scale geomechanical and hydrogeological effects of multiple CO₂
1332 injection sites on formation stability. *International Journal of Greenhouse Gas*
1333 *Control*, 5(1), pp.69–74.
- 1334 Morrow, N. and Harris, C., 1965. Capillary Equilibrium in Porous Materials. *Society of*
1335 *Petroleum Engineers Journal*, 5(1), pp.418–420.
- 1336 Müller, N., 2011. Supercritical CO₂-Brine Relative Permeability Experiments in
1337 Reservoir Rocks—Literature Review and Recommendations. *Transport in*
1338 *Porous Media*, 87(2), pp.367–383.
- 1339 Kaveh, N.S, E.S.J. Rudolph, W.R. Rossen, P. van Hemert, and K.H.Wolf, Interfacial
1340 Tension and Contact Angle Determination in Water-sandstone Systems with
1341 Injection of Flue Gas and CO₂. *IOR 2013 – 17th European Symposium on*
1342 *Improved Oil Recovery St. Petersburg, Russia, 16-18 April 2013, (April 2013),*
1343 pp.16–18.
- 1344 Nakatsuka, Y. et al., 2010. Experimental study on CO₂ monitoring and quantification
1345 of stored CO₂ in saline formations using resistivity measurements. *International*
1346 *Journal of Greenhouse Gas Control*, 4(2), pp.209–216.
- 1347 Nielsen, L.C., Bourg, I.C. and Sposito, G., 2012. Predicting CO₂–water interfacial
1348 tension under pressure and temperature conditions of geologic CO₂ storage.
1349 *Geochimica et Cosmochimica Acta*, 81, pp.28–38.

- 1350 Nordbotten, J. M., Celia, M. a., Dahle, H. K. and Hassanizadeh, S. M., 2007.
1351 Interpretation of macroscale variables in Darcy's law. *Water Resources*
1352 *Research*, 43(8).
- 1353 Nordbotten, J. M, Celia, M. A., Dahle, H. K. and Hassanizadeh, S. M., 2008. On the
1354 definition of macroscale pressure for multiphase flow in porous media. *Water*
1355 *Resources Research*, 44(6), pp.1–8.
- 1356 Nordbotten, Jan Martin, Celia, M.A. and Bachu, S., 2005. Injection and storage of
1357 CO₂ in deep saline aquifers: Analytical solution for CO₂ plume evolution during
1358 injection. *Transport in Porous media*, 58(3), pp.339–360.
- 1359 Olivella, S., Carrera, J., Gens, A. and Alonso, E., 1994. Nonisothermal multiphase
1360 flow of brine and gas through saline media. *Transport in porous media*, 15(3),
1361 pp.271–293.
- 1362 Omambia, A.N. and Li, Y., 2010. Numeric modeling of carbon dioxide sequestration
1363 in deep saline aquifers in Wangchang Oilfield-Jiangnan Basin, China. *Journal of*
1364 *American Science*, 6(8).
- 1365 Ouakad, H.M., 2013. Modeling the CO₂ Sequestration Convection Problem Using
1366 the Lattice Boltzmann Method. *Mathematical Problems in Engineering*, 2013,
1367 pp.1–10.
- 1368 Ouellet, A., Bérard, T., Desroches, J., Frykman P., Welsh, P., Minton, J., Pamukcu,
1369 Y, Hurter, S., Schmidt-Hattenberger, C., 2011. Reservoir geomechanics for
1370 assessing containment in CO₂ storage: A case study at Ketzin, Germany.
1371 *Energy Procedia*, 4, pp.3298–3305.
- 1372 Ozgur, E. and Gumrah, F., 2009. Diffusive and Convective Mechanisms during CO₂
1373 Sequestration in Aquifers. *Energy Sources, Part A*, 31(8), pp.698–709.
- 1374 Pentland, C.H., 2011. Measurements of Non-wetting Phase Trapping in Porous
1375 Media. 2010(Awarded).

- 1376 Pentland, C., El-Maghraby, R., Iglauer, S. and Blunt, M. J., 2011. Measurements of
1377 the capillary trapping of super-critical carbon dioxide in Berea sandstone.
1378 *Geophysical Research Letters*, 38(6), pp.2007–2010.
- 1379 Pickup, G.E., Stephen, K. D., Ma, J., Zhang, P. and Clark, J. D., 2005. Multi-Stage
1380 Upscaling: Selection of Suitable Methods. In D B Das & S M Hassanizadeh, eds.
1381 *Upscaling Multiphase Flow in Porous Media SE - 10*. Springer Netherlands, pp.
1382 191–216.
- 1383 Pini, R., Krevor, S.C.M. and Benson, S.M., 2012. Capillary pressure and
1384 heterogeneity for the CO₂/water system in sandstone rocks at reservoir
1385 conditions. *Advances in Water Resources*, 38, pp.48–59.
- 1386 Pistone, S., Stacey, R. and Horne, R., 2011. THE SIGNIFICANCE OF CO₂
1387 SOLUBILITY IN GEOTHERMAL RESERVOIRS. Proceedings, Thirty-Sixth
1388 Workshop on Geothermal Reservoir Engineering. Stanford University, Stanford,
1389 California, January 31 - February 2, 2011.
- 1390 Plug, W.-J. and Bruining, J., 2007. Capillary pressure for the sand–CO₂–water
1391 system under various pressure conditions. Application to CO₂ sequestration.
1392 *Advances in Water Resources*, 30(11), pp.2339–2353.
- 1393 Plug, W-J, Mazumder, S. and Bruining, J, 2006. Capillary pressure and wettability
1394 behavior of the coal-water-carbon dioxide system at high pressures.
1395 *International CBM ...*, pp.1–15.
- 1396 Preisig, M. and Prévost, J.H., 2011. Coupled multi-phase thermo-poromechanical
1397 effects. Case study: CO₂ injection at In Salah, Algeria. *International Journal of*
1398 *Greenhouse Gas Control*, 5(4), pp.1055–1064.
- 1399 Pruess, K, Bielinski , A, Ennis-King, J, Le Gallo, Y, Garcia, J, Jessen, K, Kavscek, T,
1400 Law, D H- S, Lichtner, P, Oldenburg, C, Pawar, R., Rutqvist, J, Steefel, C,
1401 Travis, B, Chin-Fu Tsang, White, S, and Tianfu., 2003. Code intercomparison
1402 builds confidence in numerical models for geologic disposal of CO₂. In J. GALE
1403 & Y. KAYA, eds. *Proceedings of the 6th International Conference on*

- 1404 *Greenhouse Gas Control Technologies, Kyoto, Japan, October, 2002.* Oxford,
1405 UK: Pergamon.
- 1406 Pruess, Karsten, Oldenburg, C.M. and Moridis, G.J., 1999. TOUGH2 User's Guide
1407 Version 2. Lawrence Berkeley National Laboratory.
- 1408 Pusch G, May F, Bernstone C, Höllwart J, Lillie J, Mundhenk N, W.H., 2010.
1409 Common Features of Carbon Dioxide and underground Gas Storage (2). *Oil*
1410 *Gas European Magazine*, 36(3/4), pp.131–136.
- 1411 Riaz, A. and Tchelepi, H.A., 2004. Linear stability analysis of immiscible two-phase
1412 flow in porous media with capillary dispersion and density variation. *Physics of*
1413 *Fluids (1994-present)*, 16(12), pp.4727–4737.
- 1414 Ritter, L.C. and Drake, R.L., 1945. Pore Size Distribution in Porous Materials.
1415 *Industrial & Engineering Chemistry Analytical Edition*, 17(12), pp. 782-
1416 786. Rutqvist, J, Wu, Y.-S., Tsang, C.-F. and Bodvarsson, G., 2002. A modeling
1417 approach for analysis of coupled multiphase fluid flow, heat transfer, and
1418 deformation in fractured porous rock. *International Journal of Rock Mechanics*
1419 *and Mining Sciences*, 39(4), pp.429–442.
- 1420 Rutqvist, J., 2011. Status of the TOUGH-FLAC simulator and recent applications
1421 related to coupled fluid flow and crustal deformations. *Computers &*
1422 *Geosciences*, 37(6), pp.739–750.
- 1423 Rutqvist, Jonny, 2012. The Geomechanics of CO₂ Storage in Deep Sedimentary
1424 Formations. *Geotechnical and Geological Engineering*, 30(3), pp.525–
1425 551. Saffman, P.G. and Taylor, G., 1958. The penetration of a fluid into a porous
1426 medium or Hele-Shaw cell containing a more viscous liquid. *Proceedings of the*
1427 *Royal Society of London. Series A. Mathematical and Physical Sciences*,
1428 245(1242), pp.312–329.
- 1429 Salimi, H., Wolf, K.-H. and Bruining, 2012. The influence of capillary pressure on the
1430 phase equilibrium of the CO₂–water system: Application to carbon sequestration
1431 combined with geothermal energy. *International Journal of Greenhouse Gas*
1432 *Control*, 11, pp.S47–S66.

- 1433 Saraji, S., Goual, L., Piri, M. and Plancher, H., 2013. Wettability of supercritical
1434 carbon dioxide/water/quartz systems: simultaneous measurement of contact
1435 angle and interfacial tension at reservoir conditions. *Langmuir: the ACS journal*
1436 *of surfaces and colloids*, 29(23), pp.6856–6866.
- 1437 Saripalli, K.P., Mcgrail, B.P. and White, Mark D, 2001. Modeling the sequestration of
1438 CO₂ in deep geological formations. In *First National Conference on Carbon*
1439 *Sequestration*. pp. 1–19.
- 1440 Schwartz, M.O., 2014. Modelling leakage and groundwater pollution in a hypothetical
1441 CO₂ sequestration project. *International Journal of Greenhouse Gas Control*, 23,
1442 pp.72–85.
- 1443 Seaton, N.A. and Walton, J.P.R.B., 1989. A new analysis method for the
1444 determination of the pore size distribution of porous carbons from nitrogen
1445 adsorption measurements. *Carbon*, 27(6), pp.853–861.
- 1446 Shafrin, E.G. and Zisman, W.A., 1960. Constitutive relations in the wetting of low
1447 energy surfaces and the theory of the retraction method of preparing
1448 monolayers¹. *The Journal of Physical Chemistry*, 64(5), pp.519–524.
- 1449 Shojai Kaveh, N., Rudolph, E. S. J., Wolf, K.-H. A. A. and Ashrafizadeh, S. N., 2011.
1450 Wettability determination by contact angle measurements: hvbB coal-water
1451 system with injection of synthetic flue gas and CO₂. *Journal of colloid and*
1452 *interface science*, 364(1), pp.237–47.
- 1453 Shukla, R., Ranjith, P., Haque, A. and Choi, X., 2010. A review of studies on CO₂
1454 sequestration and caprock integrity. *Fuel*, 89(10), pp.2651–2664. Silin, D.,
1455 Patzek, T. and Benson, S.M., 2008. A Model of Buoyancy-Driven Two-Phase
1456 Countercurrent Fluid Flow. *Transport in Porous Media*, 76(3), pp.449–469.
- 1457 Singh, P., Cavanagh, A., Hansen, H., Nazarian, B., Iding, M., and Ringrose, 2010.
1458 Reservoir Modeling of CO₂ Plume Behavior Calibrated Against Monitoring Data
1459 From Sleipner Norway. In *SPE annual technical conference and exhibition*, 19-
1460 22 September, Florence, Italy

- 1461 Solomon, S., Qin, D., Manning, M., Chen, Z., Marquis, M., Averyt, K B., Tignor, M.,
1462 Miller, H., 2007. The physical science basis. *Contribution of working group I to*
1463 *the fourth assessment report of the Intergovernmental Panel on Climate Change*,
1464 pp.235–337.
- 1465 Stanmore, B.R. and Gilot, P., 2005. Review—calcination and carbonation of
1466 limestone during thermal cycling for CO₂ sequestration. *Fuel Processing*
1467 *Technology*, 86(16), pp.1707–1743Taku Ide, S., Jessen, Kristian and Orr Jr,
1468 F.M., 2007. Storage of CO₂ in saline aquifers: Effects of gravity, viscous, and
1469 capillary forces on amount and timing of trapping. *International Journal of*
1470 *Greenhouse Gas Control*, 1(4), pp.481–491.
- 1471 Tao, Q. and Bryant, S.L., 2014. Well permeability estimation and CO₂ leakage rates.
1472 *International Journal of Greenhouse Gas Control*, 22, pp.77–87.Tiab, D. and
1473 Donaldson, E.C., 2004. *Petrophysics: Theory and Practice of Measuring*
1474 *Reservoir Rock and Fluid Transport Properties* 2nd ed., Oxford: Gulf
1475 Professional Publishing (Elsevier).
- 1476 Tian, S., Lei , G., He, S. and Yang, L., 2012. Dynamic effect of capillary pressure in
1477 low permeability reservoirs. *Petroleum Exploration and Development*, 39(3),
1478 pp.405–411.
- 1479 Tokunaga, T.K., Wan, J. Jung, J-W, Kim, T.K., Kim, Y., Dong, W., 2013. Capillary
1480 pressure and saturation relations for supercritical CO₂ and brine in sand: High-
1481 pressure P_c (S_w) controller/meter measurements, and capillary scaling
1482 predictions. *Water Resources Research*.
- 1483 Topp, G.C., Zebchuk, W. D., Davis, J. L., and Bailey, W. G., 1984. The
1484 measurement of soil water content using a portable TDR hand probe. *Canadian*
1485 *Journal of Soil Science*, 64(3), pp.313–321.
- 1486 Tsang, Chin-Fu, Birkholzer, J. and Rutqvist, Jonny, 2007. A comparative review of
1487 hydrologic issues involved in geologic storage of CO₂ and injection disposal of
1488 liquid waste. *Environmental Geology*, 54(8), pp.1723–1737.

- 1489 Vilarrasa, V., Bolster, D., Olivella, S. and Carrera, J., 2010. Coupled
1490 hydromechanical modeling of CO₂ sequestration in deep saline aquifers.
1491 *International Journal of Greenhouse Gas Control*, 4(6), pp.910–919.
- 1492 Vinegar, H.J. and Waxman, M.H., 1987. In-situ method for determining pore size
1493 distribution, capillary pressure and permeability. U.S. Patent No. 4,644,283.
1494 Washington, DC: U.S. Patent and Trademark Office.
- 1495 Virnovsky, G.A., Skjaeveland, S. M., Ingsoy, P., Norge, E. and Surdal, J., 1995.
1496 Steady-State Relative Permeability Measurements Corrected for Capillary
1497 Effects. *SPE Journal*, (3), pp.85–95.
- 1498 Wang, S., Edwards, I.M. and Clarens, A.F., 2012. Wettability phenomena at the co2-
1499 -brine--mineral interface: Implications for geologic carbon sequestration.
1500 *Environmental science & technology*, 47(1), pp.234–241.
- 1501 Wang, W. and Kolditz, O., 2007. Object-oriented finite element analysis of thermo-
1502 hydro-mechanical (THM) problems in porous media. *International journal for*
1503 *numerical methods in engineering*, 69(1), pp.162–201.
- 1504 Wang, Y., Zhang, C., Wei, N., Oostrom, M., Wietsma, T., Li, X., Bonneville, A., 2013.
1505 Experimental study of crossover from capillary to viscous fingering for
1506 supercritical CO₂-water displacement in a homogeneous pore network.
1507 *Environmental science & technology*, 47(1), pp.212–8.
- 1508 Water, M., Abaci, S., Whittaker, N., 2006. Relative permeability measurements for
1509 two phase flow in unconsolidated sands. *Mine Water and the Environment*,
1510 26(2), pp.12–26.
- 1511 White, D., Burrowes, G., Davis, T., Hajnal, Z., Hirsche, K., Hutcheon, I., Majer, E.,
1512 Rostron, B., Whittaker, S., 2004. Greenhouse gas sequestration in abandoned
1513 oil reservoirs: The International Energy Agency Weyburn pilot project. *GSA*
1514 *today*, 14(7), pp.4–11.
- 1515 White, M.D., 2002. Example Problem 9 Simulation of supercritical CO₂ into a deep
1516 saline aquifer. , pp.1-12. Pacific Northwest Laboratory.

- 1517 White, M.D., McGrail, B. P., Gale, J. and Kaya, Y., 2003. *Numerical Investigations of*
1518 *Multifluid Hydrodynamics During Injection of Supercritical CO₂ into Porous*
1519 *Media,*
- 1520 White, Mark D and McGrail, B Peter, 2005. Stomp (subsurface transport over
1521 multiple phase) version 1.0 addendum: ECKEQUILIBRIUM
1522 conservationkinetic equation chemistry and reactive transport. *Pacific Northwest*
1523 *National Laboratory, PNNL-15482, Richland, Washington.*
- 1524 White, SP, Weir, G. and Kissling, W.M., 2001. Numerical simulation of CO₂
1525 sequestration in natural CO₂ reservoirs on the Colorado Plateau. *This volume,*
1526 (64).
- 1527 Wielopolski, L. and Mitra, S., 2010. Near-surface soil carbon detection for monitoring
1528 CO₂ seepage from a geological reservoir. *Environmental Earth Sciences*, 60(2),
1529 pp.307–312.
- 1530 Woods, E.G., Comer, A.G. and others, 1962. Saturation distribution and injection
1531 pressure for a radial gas-storage reservoir. *Journal of Petroleum Technology*,
1532 14(12), pp.1–389.
- 1533 Van Wunnik, J.N.M. and Wit, K., 1989. A simple analytical model of the growth of
1534 viscous fingers in heterogeneous porous media. In: 1st European Conference
1535 on the Mathematics of Oil Recovery. University of Cambridge
- 1536 Xu, T., Sonnenthal, E., Spycher, N. and Pruess, K., 2006. TOUGHREACT—A
1537 simulation program for non-isothermal multiphase reactive geochemical
1538 transport in variably saturated geologic media: Applications to geothermal
1539 injectivity and CO₂ geological sequestration. *Computers & Geosciences*, 32(2),
1540 pp.145–165.
- 1541 Yortsos, Y.C. and Hickernell, F.J., 1989. Linear stability of immiscible displacement
1542 in porous media. *SIAM Journal on Applied Mathematics*, 49(3), pp.730–748.

- 1543 Zahid, U., Lim, Y., Jung, J. and Han, C., 2011. CO₂ geological storage: A review on
1544 present and future prospects. *Korean Journal of Chemical Engineering*, 28(3),
1545 pp.674–685.
- 1546 Zakkour, P. and Haines, M., 2007. Permitting issues for CO₂ capture, transport and
1547 geological storage: A review of Europe, USA, Canada and Australia.
1548 *International Journal of Greenhouse Gas Control*, 1(1), pp.94–100.
- 1549 Zhang, C., Oostrom, M., Wietsma, T. W., Grate, J. W. and Warner, M. G., 2011.
1550 Influence of Viscous and Capillary Forces on Immiscible Fluid Displacement:
1551 Pore-Scale Experimental Study in a Water-Wet Micromodel Demonstrating
1552 Viscous and Capillary Fingering. *Energy & Fuels*, 25(8), pp.3493–3505.